United States
Environmental Protection
Agency

Office of Transportation
and Air Quality

EPA420-D-04-002
March 2004

Advanced Technology Vehicle Modeling in PERE

EPA420-D-04-002
March 2004

Advanced Technology Vehicle Modeling in PERE

Edward Nam

Assessment and Standards Division
Office of Transportation and Air Quality
U.S. Environmental Protection Agency

NOTICE
This Technical Report does not necessarily represent final EPA decisions or positions. It is intended to present technical analysis of issues using data that are currently available. The purpose in the release of such reports is to facilitate an exchange of technical information and to inform the public of technical developments.

Table of Contents

Executive Summary

This study proposes a modeling methodology for light duty advanced technology vehicles including those powered by:

- Advanced gasoline internal combustion engine
- Advanced diesel internal combustion engines
- Hybrid electric and gasoline/diesel powertrains
- Hydrogen fuel cell hybrid

The model called PERE (Physical Emission Rate Estimator) is designed to support the new EPA energy and emissions inventory model, MOVES (MOtor Vehicle Emissions Simulator). PERE is a stand-alone spreadsheet, which can be run by an informed user. It outputs Pump-to-Wheel (PTW) fuel consumption rates. The purpose of PERE is to fill data gaps in MOVES and to help it extrapolate to future projections of energy and emissions. The current version of PERE will model many of the advanced technologies in MOVES and is capable of capturing more. If the user is knowledgeable of the vehicle parameters required in PERE, other technologies can be modeled that are not described in this report (e.g. series hybrids etc.). However, since PERE requires significant development time for each technology, the current version of MOVES (2004) may directly model some vehicles using modifications to existing rates (e.g. hydraulic hybrids and some alternative fuels).

MOVES is currently being integrated with GREET (developed at Argonne Laboratory), which produces upstream Well-to-Pump (WTP) energy and emissions rates. The combination of PERE, MOVES, and GREET will provide a powerful comprehensive modeling suite for anyone requiring emissions inventory projections or life cycle (energy/emissions) studies for mobile sources into the future.

As the name implies, PERE uses physical principles to model propulsion systems in the vehicle. It is therefore built on a relatively strong foundation. The model is based on a sound, yet elegantly simple model for the internal combustion engine. Simulation of hybridization is achieved by inserting a secondary power source (usually a battery/motor combination). Fuel cell vehicles are simulated by replacing the engine with an aggregate fuel cell system. PERE takes vehicle input parameters, then runs the vehicle through driving cycles defined by the user and outputs second-by-second fuel consumption rates. All of the processes are transparant to the user, which allows for easy updates.

The model is validated to four production conventional gasoline, and five advanced (and hybrid) vehicles by comparing the PERE output to the rated fuel economy figures. The advanced vehicles include advanced engine technologies, such as lean burn gasoline. The model performs well, in most cases the predictions are within 10%, as the figure below shows.

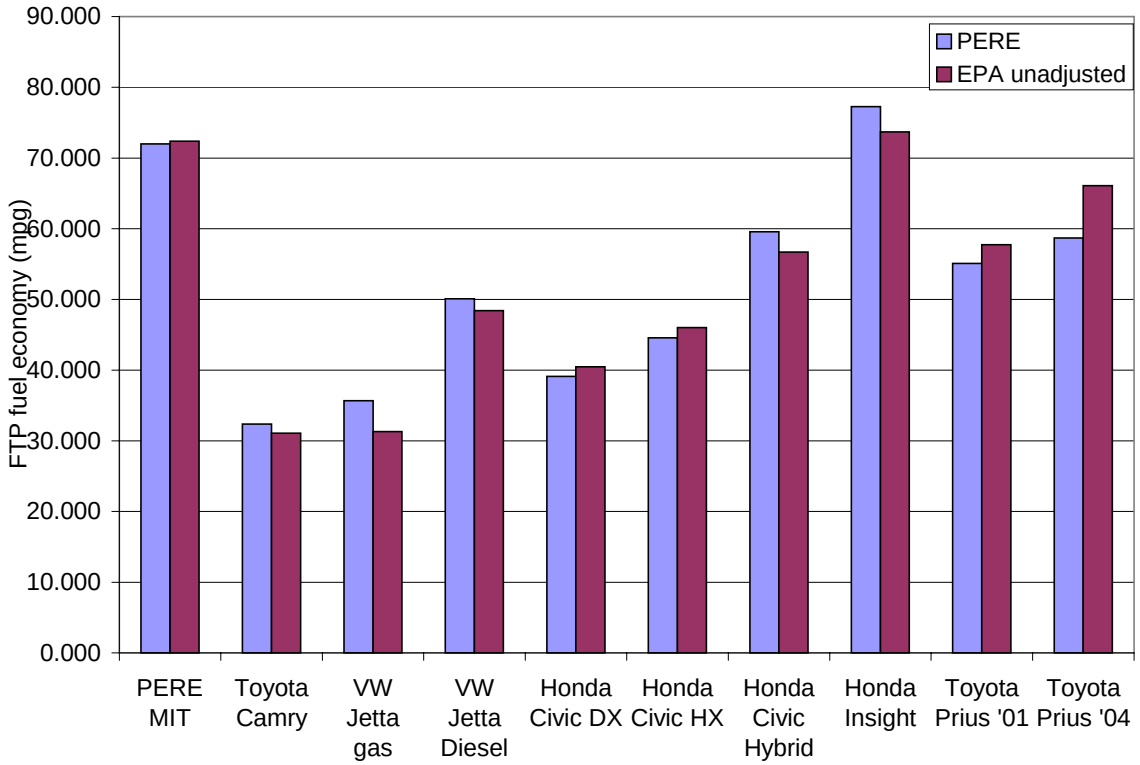

Figure ES1. Combined fuel economy (city/highway) estimates from PERE compared to vehicle rated values.

The fuel cell model describes a direct hydrogen PEM fuel cell hybrid. It is validated to the fuel economy results from the Honda FCX vehicle. The model predicts fuel economy within 5% of the measured value.

The report also includes a sensitivity analysis, which will help guide users to determine which parameters require more accuracy.

Finally, the report describes how PERE might be used to support MOVES. It provides guidance for how parameters may be estimated in order to perform future projections. It also describes a methodology by which the PERE output can be integrated into MOVES.

Introduction

From reading manufacturer press releases, and seeing the new vehicles being offered, it is becoming evident that advanced technology vehicles, such as hybrids, will become more commonplace in the near future. A hybrid vehicle combines two forms of propulsion in order to optimize efficiency and fuel economy. The incremental cost of hybrid vehicles is expected to decrease as volumes increase, and as public acceptance increases. There are also other types of advanced vehicles, such as clean diesel, and fuel cell vehicles, which may claim a portion of the market in the future. It is important to understand the possible effects that these vehicles will have on the fleet and the environment.

The goal of this project is to develop a model, which can simulate a variety of future or advanced technology vehicles for the purpose of supporting policy analysis within EPA as well as estimating future emissions inventories. The Physical Emissions Rate Estimator (or PERE) is expected to generate fuel (or energy) consumption rates for the new EPA emissions inventory model, MOVES (MOtor Vehicle Emission Simulator). PERE is in a spreadsheet format and should be usable for most users, who have a nominal amount of background information on hybrids and fuel cells.

The current report describes the modeling of fuel and energy consumption by conventional and advanced technology light duty vehicles using physical principles. The model development and validations are for the following light duty technology types: conventional gasoline, advanced gasoline (lean burn), diesel, “mild” parallel hybrid, “full” parallel hybrid, and fuel cell hybrid vehicles. With the exception of fuel cells, these are the technologies, which have the most short-term promise, i.e. they are already sold in significant numbers and are likely to experience growth. The number of other advanced technology combinations that could exist are enormous. Such examples are hydraulic hybrids, series hybrids, plug-in hybrids, hydrogen internal combustion engine, pure electric, etc. This report does not model all of the possible combinations, however the hope is to demonstrate that PERE is a robust model that can accommodate most of these technologies if the need arises.

Though the model is based on mathematical and physical principles, it is intended to be aggregate, and is probably not appropriate for engineering or product development. Thus it is designed to model a typical vehicle of technology type, rather than a specific vehicle. Energy flows within vehicle components are modeled using overall systems efficiencies. The validations in this report are conducted with certification fuel economy data. Where appropriate, simplifications and approximations are made using physical constraints, or based on publications in the literature.

For the purposes of modeling the future fleet, our goal is to allow as many of the significant assumptions as possible to be under the control of the user. However, default values will be presented in this paper. An attempt will be made to justify the assumptions in each case.

The report begins by describing conventional vehicles, both gasoline and diesel. It then goes on to briefly examine advanced engines. Hybrid vehicles are modeled and validated followed by

fuel cell vehicles. The report caps off with a sensitivity analysis and describes how PERE rates might feed into MOVES.

The final form that the model takes for the integration may be different from what is presented in this report.

Conventional Vehicles

Vehicle Model

As Figure 1 shows, the model is basically a "backwards-looking" model in that it takes a driving cycle (second-by-second speed vs. time) input and outputs the energy consumption required to follow the drive trace. The power demand is based on overcoming inertia, road grade, tire friction, and aerodynamic loss. This is essentially the VSP equation shown in numerous publications.

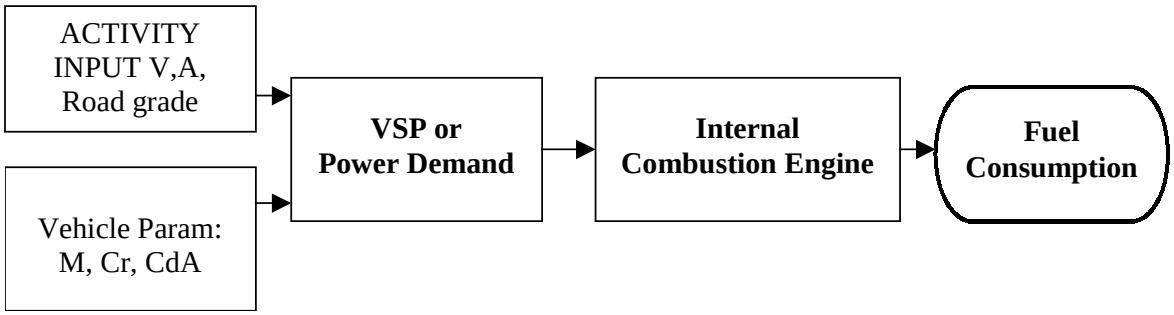

Figure 1.Conventional internal combustion engine vehicle model flow.

The power demand (in Watts) is the brake power or, VSP*m:

$$P_b = VSP*m = mv[a(1+\varepsilon) + g*grade + gC_R] + 0.5\rho C_D A_r v^3 \quad (1)$$

where:

v: is vehicle speed (assuming no headwind) in m/s (or mps)
a: is vehicle acceleration in m/s^2
ε: is mass factor accounting for the rotational masses (~0.1)
g: is acceleration due to gravity (9.8 m/s^2)
grade: is road grade
C_R: is rolling resistance (~0.009)
ρ: is air density (~1.2 kg/m^3)
C_D: is aerodynamic drag coefficient (~0.30)
A_r: is the frontal area in $meters^2$ (~2.4 m^2)
m: is vehicle mass in metric tonnes.

The rotating mass term, ε, is assumed to be 0.1 [Jimenez, 1999]. However it increases at lower gears [Gillespie, 1992]. The rolling resistance for radial tires, C_R, can range from 0.008 – 0.013 for a majority of the on- road passenger car tires. This value can be larger depending on state of inflation, temperature, ground surface type, and speed (though this effect is minor) [Bosch, 2000; Gillespie, 1992]. Heavy-duty trucks tend to have lower resistance. The aerodyanamic drag, C_D,

varies according to the body shape, and is sometimes provided by the manufacturers. The frontal area, A_r, of the vehicle is also sometimes supplied. Where it is unknown, PERE uses 93% of the box frontal area based on a number of vehicles examined by the author. This is calculated using the dimensions available for the vehicles:

$$A_r = (H-GC)*W*0.93 \quad (2)$$

where: H is the vehicle height
GC is the ground clearance
W is the width.

Alternately to Equation 1, one could also use:

$$P_b = Av + Bv^2 + Cv^3 + mv[a + g*grade] \quad (3)$$

where the coastdown coefficients: A, B, C, are rolling, rotating and aerodynamic resistive coefficients, respectively. These are determined from track coast-down tests and are available from the EPA certification database. The "A" coefficient is equivalent to the tire rolling resistance terms of Equation 1. "B" tends to be small, and describes higher order rolling resistance factors in addition to rotating friction losses. The "C" term represents the air drag coefficient terms. These two equations are not necessarily identical, and it is possible that by preferring Equation 1 over 3, that PERE could overestimate fuel economy (underestimate energy consumption) somewhat. When available, the coastdown (track) coefficients should be used in Equation 2, since the road load is closer to the test conditions. This will be discussed in greater detail in the sensitivity section.

Gasoline Spark Ignited Internal Combustion Engine

The internal combustion engines (ICE) converts chemical into mechanical energy. This combustion process, as well as the losses inherent to it, is a critical element to the modeling of vehicles. Modern vehicles powered with gasoline have been the subject of several models in the literature. This paper remains consistent with the approach developed by Ross and An [1993]; Barth et al. [1999]; and Weiss et al. [2000] as well as other authors. The formalism is described well in Ross [1997], which will be briefly reviewed here.

The basis for the engine model lies in the linear relationship between brake power and fuel consumption, both represented in mean effective pressure (mep in bar) units. The power equivalent of fuel is:

$$P_f = FR*LHV \quad (4)$$

where FR is the fuel consumption rate in grams per second
LHV is the lower heating value of the fuel (approximately 43.7 kJ/g for gasoline)

In mep [kPa], this becomes:

$$\text{fuel mep} = 2000*P_f/(VN) \quad (5)$$

where V is the engine displacement in liters
N is the engine speed (rps)

One can model it as follows:

$$\text{Fuel mep} = k + \text{bmep}/\eta \quad (6)$$

or

$$\text{fuel mep} = (\text{fmep} + \text{bmep})/\eta \quad (7)$$

where k is the engine friction related term (in friction mep terms, k = fmep/η) and η is a measure of the indicated or thermal efficiency of the engine, i.e., it is the fraction of the energy in the fuel which is converted to useful work. This efficiency describes engine properties such as compression ratio, fuel mixing, fuel type, cylinder temperature, valve timing, spark timing, combustion chamber geometry, etc. [Muranaka, 1987; Ross, 1997]. Ideally, this is limited by engine heat cycle and thermodynamic 2nd law losses at the upper limit.

The indicated thermal efficiency is not to be confused with "mechanical" efficiency, or even with "overall" engine efficiency (discussed below). k and fmep reflect the mechanical losses in the engine mainly from rubbing, pumping, and auxiliary load losses. Specifically, the rubbing losses can originate from valves, gears, piston rings, lubricant, piston, crankshaft, etc [Milington & Hartles, 1968]. The pumping losses are derived from the difference between the intake cylinder and ambient pressures. The throttle plate, and intake, exhaust and valve geometry on gasoline engines cause this loss in "volumetric efficiency" [Patton, et al., 1989]. As an engine "breathes" better, the pumping losses decrease and its volumetric efficiency increases. Thus an engine with 4 valves per cylinder is typically more fuel efficient than one with 2 valves. Also diesel engines lack throttle plates, so they have improved volumetric efficiency over gasoline engines. Throttling results in about 25% of the friction losses [Ross, 1997]. The product of mechanical efficiency (which we have not quantified yet) and thermal efficiency is the overall engine efficiency, which will be discussed in more detail below.

Given the fuel mep, to obtain a mass fuel rate, one only needs engine displacement and speed. The bmep, is equivalent to brake power and can be determined from road load using the ubiquitous road load Equations 1 & 3. Equation 7 is equivalent to the one used by Weiss , et al. [2000]:

$$\text{imep} = \text{fmep} + \text{bmep} \quad (8)$$

where imep is the indicated mep equivalent to fuel mep*η.

This relationship has been plotted on Figure 2 below for a series of 10 different engines at many different operating conditions, where the wide-open throttle points have been omitted [Nam & Sorab, 2004]. According to the figure the indicated or thermal efficiency (inverse slope) is η ~ 0.40, while k ~ 4.24 bar and fmep ~ 1.72 bar for this diverse family of engines. This procedure for estimating the engine friction analytically is referred to as the "Willans Line" method [Millington & Hartles, 1968]. It is similar to experimentally motoring the engine down. The largest uncertainty associated with this methodology lies in the slight curvature of the lines

especially at high load. This is why the high load points were omitted, though there is still some curvature [Pachernegg, 1969]. Despite the limitations, the method is quite robust as the lack of scatter in Figure 2 demonstrates. For the scale of modeling in this report, this estimate is quite sufficient.

It has been found that the indicated efficiency has not changed significantly over the preceding 3 decades [Nam & Sorab, 2004, Weiss, et al. 2000]. It should be noted that this holds for engines operating at stoichiometry, where there is exactly the right quantity of air to combust the fuel completely. Older vehicles can run rich under various high power driving conditions, and those need to be modeled separately [Goodwin, 1996]. It is assumed that present and future vehicles (which have to meet SFTP standards) will not undergo significant periods of enrichment. However future vehicles may have improved efficiency if lean burn engines (or other advanced technologies) become more prevalent (this will be discussed more later).

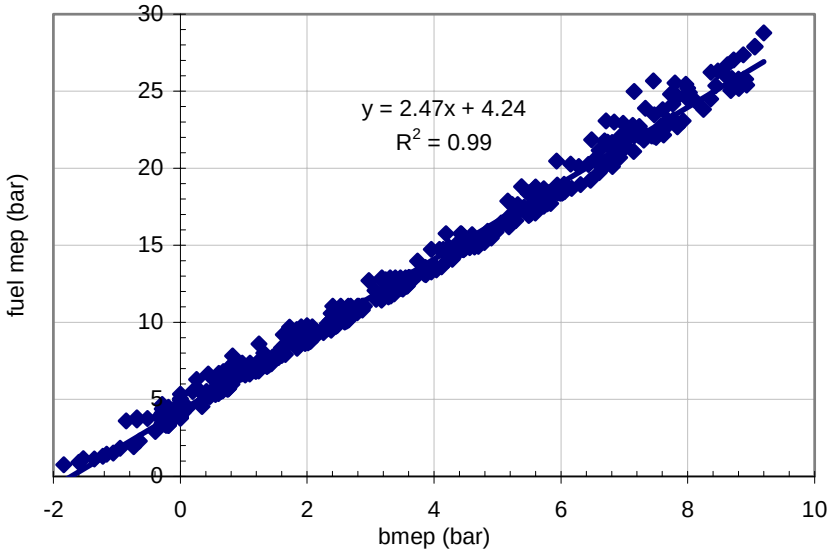

Figure 2. Fuel mean effective pressure as a function of brake mep for 10 engines from 4 different manufacturers, omitting wide open throttle points [Nam & Sorab 2004].

It was mentioned earlier that “indicated thermal” efficiency is NOT the same as “overall” engine efficiency. The latter includes the effect of mechanical or frictional losses. This can be demonstrated most dramatically in Figure 2. The overall (or “brake”) efficiency of the engine at a given operating (load) point, is the x-axis value (output energy) divided by the y-axis value (input energy). For example, at bmep = 2 bar, the fuel mep = 10 bar, meaning the overall engine efficiency is 20%. Also at bmep = 8 bar, fuel mep = 24 bar, meaning the engine efficiency is 33%. It is clear that the overall efficiency increases with the load (omitting wide-open throttle and fuel enrichment) while the indicated thermal efficiency (inverse slope) remains constant at roughly 40%. Thus the indicated efficiency is the efficiency limit of the engine. The product of the indicated and mechanical efficiency is the overall engine efficiency. Thus the mechanical efficiency is dependent on load and engine speed, and the most efficient operating points are those with low engine speed and high load. This highlights the advantage that hybrids have over conventional vehicles: the engine operates more at higher loads and thus higher efficiencies, while the battery (or other energy storage medium) operates during low engine efficiency modes

(allowing it to shut down). To calculate a final overall vehicle (or "pump-to-wheel" efficiency, it is also necessary to factor in transmissions and final drive losses. Accessories can also play a minor role.

Though the scatter in Figure 2 is small, there is some systematic relationship, which can explain some of the variation. It is well known that the friction (or offset) is dependent on the engine speed. This is demonstrated in Figure 3. The base friction term can thus be modeled

$$k = k_0 + k_1 N \tag{9}$$

where: k_0 = 3.283 bar and k_1 = 0.000515 bar/rpm for the present gasoline engines (multiply by 100 to get kPa, then divide by 2000 to get the proper units for the fuel rate equation). The friction at idle is significantly higher (about 50%). There is a slight curvature evident in the figure and some references include higher order terms, but these are more necessary for higher revving engines [Yagi, et al., 1990].

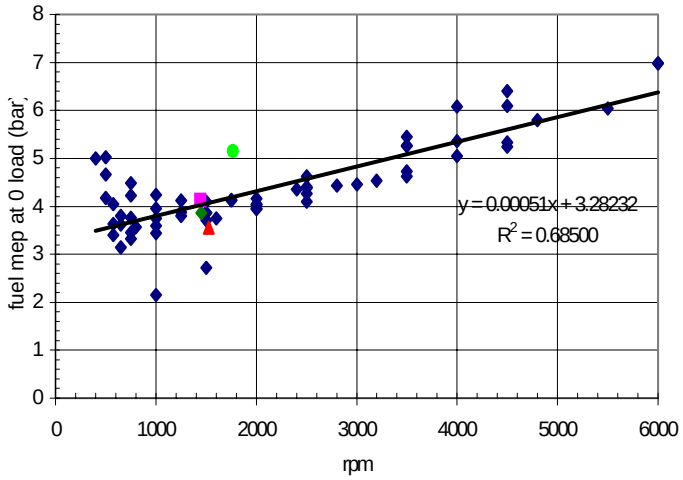

Figure 3. Engine friction as a function of engine speed for 10 engines. [Nam & Sorab 2004].

Though the indicated efficiency has changed little over the years, the friction has decreased over the past 30 years at a rate of roughly 10% per decade [Nam and Sorab, 2004; Sandoval and Heywood, 2003]. Various technologies have helped accomplish this: overhead cam, multiple valves per cylinder, improved lubricants, variable valve timing, etc. Additionally, engine efficiency can be improved with "advanced" technologies such as lean burn gasoline (e.g., Honda HX), Atkinson cycle (as in Toyota Prius), Direct Injection Spark Ignition (DISI – no current model in US), Homogeneous Charge Compression Ignition (HCCI), or with variable compression ratio. Fuel economy can also be improved with variable displacement, cylinder deactivation, or adding a turbocharger with engine downsizing in the future. There may come a day when engines will be "variable everything". Some of these technologies will be discussed further below.

Despite the many different models and manufacturers of gasoline engines (neglecting advanced engines), there is remarkable homogeneity in their performance characteristics (within a certain

threshold). As a result, it is possible to develop "rules of thumb", which give rough estimates, of engine efficiency, friction, peak torque and peak power, given only its displacement (and model year). Figure 4 shows generic peak torque and power curves for a 2.0 liter gasoline engine [Weiss et al., 2000]. The curves can be scaled to different engine sizes using relationships in Sandoval and Heywood [2000]. While not all 2.0 liter engines will have the same shape and peak values, the general trends appear in most engines and this relationship is sufficient for our modeling needs. These peak curves are mainly used to determine transmission down-shift points and for cut-point determination for hybrids (where engines may be significantly downsized), therefore the PERE output is not highly sensitive to the shape of the curves.

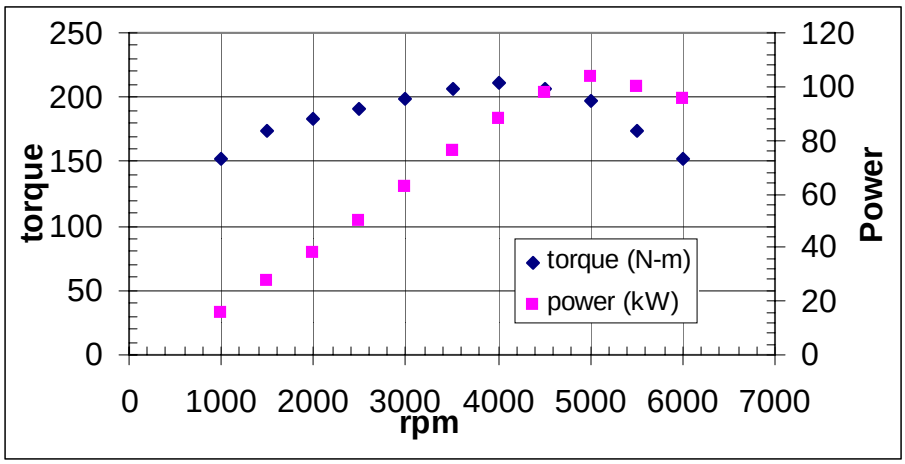

Figure 4. Engine peak torque and power for a "generic" 2.0L gasoline engine.

Transmission

Another element required to calculate total vehicle efficiency is transmission and final drive efficiency. All vehicle powerplants must connect to the wheels via a transmission. Sometimes this is as simple as a single gear reduction (as in many fuel cell and electric vehicles). More often though, there are multiple gears to take advantage of the engine's limited operating range. The multi-gear transmission model used for PERE is based on Thomas and Ross [1997]. While transmissions and their shift strategies vary tremendously between vehicles, the overall fuel consumption rate is not highly sensitive to this sub-model as long as 'sensible' parameters are employed.

The engine speed is:

$$N = (N/v)_{top}*(60rps/rpm)*(g/g_{top})*v \qquad (10)$$

where N is engine speed in rps
$(N/v)_{top}$ is the rpm to speed ratio in top gear
v is vehicle speed in mph
(g/g_{top}) is the gear ratio at the various gears

Typical values (with shift points) are shown in tables in Appendix B. $(N/v)_{top}$ is assumed to be a constant, but a future version of PERE may make it dependent on engine size. Smaller engines

tend to rev higher than larger engines. One could also calculate engine speed from final drive ratio and tire radius.

In order to meet the power demand of some driving cycles, it is necessary to downshift. The algorithm for downshifting is as follows:

If TorqueDemand > MaxTorque
    Then Downshift

The algorithm is repeated until the Torque demand is met, or gear 1, whichever comes first. There is no consideration for shift or ride quality in this simplified model.

All the multi-gear vehicles in this study are assumed to be 5-speed manual transmission for simplification. The overall efficiency used by PERE for a manual transmission is approximately: $\eta_{trans} = 0.88$, which includes final drive losses [Thomas & Ross, 1997; Weiss et al., 2000]. Typical auto transmission efficiency would be about 75% using a single value. There is additional significant loss in automatic transmissions during gear shifts, due to the slippage in the torque converter. The model could be slightly improved by making the efficiency dependent on load and/or rpm [Park, et al., 1996].

Manual transmissions range in efficiency from 87-99%. Automatic transmissions range 85 – 95% when locked, but can drop to 60 - 85% unlocked. An overall 1.5% improvement in transmission efficiency could correspond to a 0.1 km/L increase in fuel economy [Greenbaum, et al., 1994; Kluger, et al., 1995; Bishop, et al., 1996]. Manual transmissions have similar efficiencies to continuously variable transmissions (CVT), so can be seen as equivalent to advanced transmissions.

Vehicles whose drivetrains run off of motors do not require complex transmissions employing gear shifts. These motor driven vehicles usually only require a single gear due to the large operating range of motors. Single gear transmissions naturally tend to be very efficient and are assumed to be 95% efficient in this report.

If transmissions efficiency is added to Equations 4 through 6, we would obtain the fuel rate equation used in PERE [Nam, 2003]:

$$FR = \varphi\,[kNV + (P_b/\eta_t + Pacc)/\eta] / LHV \qquad (11)$$

where

- φ: is the fuel air equivalence ratio (mostly =1)
- k: is the engine friction (can depend on engine speed).
- N: is the engine speed, depending mostly on vehicle speed
- V: is the engine displacement volume
- η_t: is a transmission and final drive efficiency (~0.88)
- η: is a measure of the engine indicated efficiency (~0.4).
- Pacc: is the power draw of accessories such as air conditioning. This is a function of ambient temperature, T, and humidity (and engine speed for AC). Without AC, it is some nominal value ~ 0.75kW.

LHV: is the factor lower heating value of the fuel (~43.7kJ/g).

Diesel Internal Combustion Engine

Diesel engines are different from gasoline engines in several important ways. They run on diesel fuel, which has higher density, energy density, and carbon content. The fuel is self-ignited by compression rather than with a spark (hence it is also known as compression ignition engine). The increase in compression ratio required for compression ignition improves the thermal efficiency. The engines can also combust fuel in an environment that is lean of stoichiometry. A stoichiometric fuel air mixture has just enough air to completely combust (or oxidize) all of the fuel, so a lean mixture has more air, and rich mixture has more fuel. Naturally, lean mixtures result in higher fuel efficiency. Modern diesel engines inject the fuel directly in the chamber with electronically controlled bursts, which increases the pumping efficiency (decreases friction) by doing away with the losses inherent to a throttle. Unfortunately, diesel engines have higher NOx and particulate matter (PM) emissions. The excess NOx emissions is due to the lack of aftertreatment system, and the PM emissions is due to the combustion mechanism with fuel droplets. Advanced diesel engines complying with federal Tier 2 emission standards will require aftertreatment technologies, which may require the fuel combustion to run at stoichiometry on occasion so that NOx and PM can be stored, then treated. This will in turn, have a small negative effect on fuel economy.

In PERE, Diesel indicated efficiency is assumed to be 0.45. This is 12.5% more efficient than current gasoline engines [Wu & Ross 1997]. Weiss et al. [2000] employ an indicated efficiency of 0.51 for advanced diesel engines.

The friction in diesel engines is typically lower than their gasoline counterparts [Heywood, 1988, Weiss, et al., 2000, Wu&Ross 1997] – though this is mostly in the speed independent term (k_0 in Eq. 8). However, Ball et al. [1986] measured a diesel engine to have similar (total) friction compared to an equivalent gasoline engine at higher operating conditions. In a diesel engine, the pumping losses are significantly lower, but the piston/crank assembly as well as auxiliary load (mainly from high pressure fuel injector) losses are higher. This hints that the speed dependent term (k_1) should be higher for diesels, or that higher order terms in Equation 9 are necessary. For PERE, we assume that k_0 is 25% lower, which is consistent with many of the references above, but we also assume that k_1 is higher (~.00072 bar/rpm) to match overall friction at higher speeds. Whatever the particular values chosen for k_1, this is a small correction to the output fuel consumption rate (see Figures 2 & 3). The output is not be very sensitive to this term.

The transmission model for diesel powertrains is identical to that described above, with the exception that diesel engines tend to rev lower. The $(N/v)_{top}$ is estimated to be 75% that of gasoline. This figure is obtained by comparing peak rpm power values from an assortment of vehicles, which have a diesel option (US and European). E.g. VW Jetta, VW Beetle, Ford Focus, Ford Mondeo, & Peugeot 607. See Table 1.

The peak torque and power curves are generically determined by Weiss et al. [2000]. Figure 5 shows the relationship for a 2.0L turbocharged diesel. The torque curves are flatter than that of gasoline engines. This high low-end torque gives diesel engines the advantage in towing as well

as decent 0-30 mph acceleration compared to their naturally aspirated gasoline equivalents (of same displacement). However the peak power tends to be lower, thus the overall 0-60 mph acceleration may be lower depending on the vehicle.

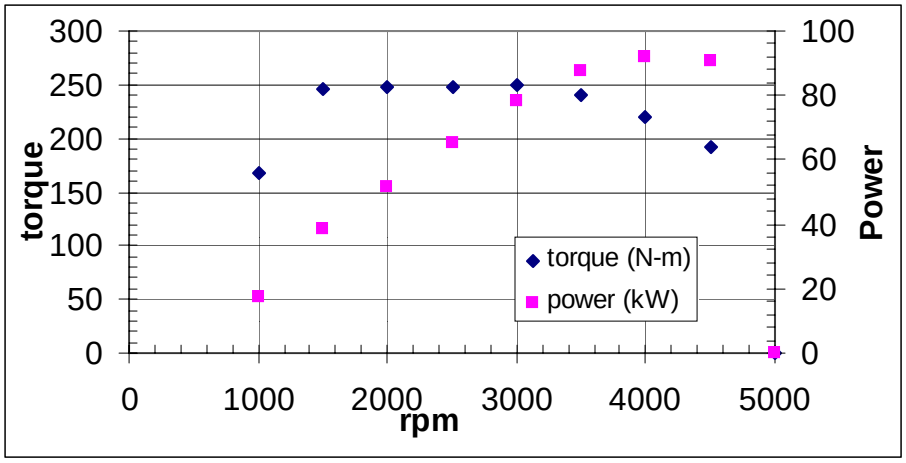

Figure 5. The peak torque and power curves for a "generic" 2.0L diesel engine.

Diesel engines are ideally suited for turbo charging. A turbo charger employs the exhaust heat energy to spin a turbine, which pumps more air charge into the engine cylinders. This efficient use of energy generates more power with a smaller engine. As a result virtually all light and heavy duty diesels employ turbo chargers. Unfortunately, the variety of turbocharger sizes makes generating peak torque and power curves, given only engine displacement, a difficult exercise. This would matter more if we were constructing the model using a performance basis (e.g. 0-60 mph time), rather than a fuel economy basis.

It is useful to conduct a comparison of gasoline and diesel light duty vehicles currently sold. Comparing the current technologies can help us to extrapolate how they will compare in the future. Table 1 shows the power and weight of various vehicles in the American and European markets.

Based on the table, we note that diesel engines tend to be heavier than their gasoline counterparts (to accommodate higher pressures), thus they often need to be downsized in order to fit into the same frame. According to the ratios of these same vehicles, the turbocharged diesel engines should be approximately 5% smaller. Due to the many differences between gasoline and diesel engines, it is impossible to do a perfect apples-to-apples comparison. However, based on these vehicles, the equivalent vehicle weight of a diesel is assumed to be 4% higher than the gasoline vehicle.

Table 1. Diesel vehicles used for comparison

model	max torque	max power	displacement (l)	curb weight (kg)
Ford Focus Diesel	200N-m@ 2000rpm	66kW@ 4000rpm	1.753	1258
Ford Focus Gasoline	160Nm@ 4400rpm	85kW@ 5500rpm	1.8	1200
Ford Mondeo Diesel	245N-m@ 1900rpm	85kW@ 4000rpm	1.998	1498
Ford Mondeo Gasoline	190Nm@ 4500rpm	107kW@ 6000rpm	1.999	1376
peugot 607 diesel	250N-m@ 1750rpm	79kW@ 4000rpm	1.997	1500
peugot 607 gasoline	217Nm@ 3900rpm	116kW@ 5650rpm	2.231	1455
VW Beetle Diesel	210N-m@ 1900rpm	66kW@ 3750rpm	1.896	1270
VW Beetle Gasoline	172Nm@ 3200rpm	85kW@ 5400rpm	1.984	1222
VW Jetta Diesel	240Nm@ 1800rpm	75kW@ 4000rpm	1.9	1347
VW Jetta Gasoline	165Nm@ 2600rpm	86kW@ 5200rpm	2.0	1331

* All sources are either from manufacturer website, Car&Driver, or Road&Track

Advanced Internal Combustion Engine (ICE)

In this report “advanced” technology is defined as a vehicle (or component) that is improved over those in most vehicles currently. Advanced ICE vehicles might employ one or more non-standard engine or driveline technologies meant to improve thermal, and/or driveline efficiencies, in order to improve fuel economy and performance. Examples include: lean-burn gasoline engines, variable displacement, direct injection gasoline, and continuously variable transmission (CVT).

In order to model future vehicles, it is educational to study current technologies comparing them with their predecessors. Two areas which have seen marked improvement in the past, are engine friction and power. The former likely leading to the latter. Typically, improvements in (overall) engine efficiency can either improve fuel economy, or increase engine size in order to increase power performance (thus maintaining the same fuel economy). The latter has been the main trend over the past few decades, though there is evidence to show that specific power (power per unit displacement) has also improved [Chon and Heywood, 2000].

Based on the research of Chon and Heywood [2000] the relationship between engine power and model year has been established for the past 15 years. This trend has been projected forward by Weiss et al. [2000] and is shown in Figure 6. The friction reduction projections have also been added to the figure, based on the research of Sandoval and Heywood [2003] and Nam and Sorab [2004]. Advanced diesel trends are assumed to be the same, though their starting values may be different.

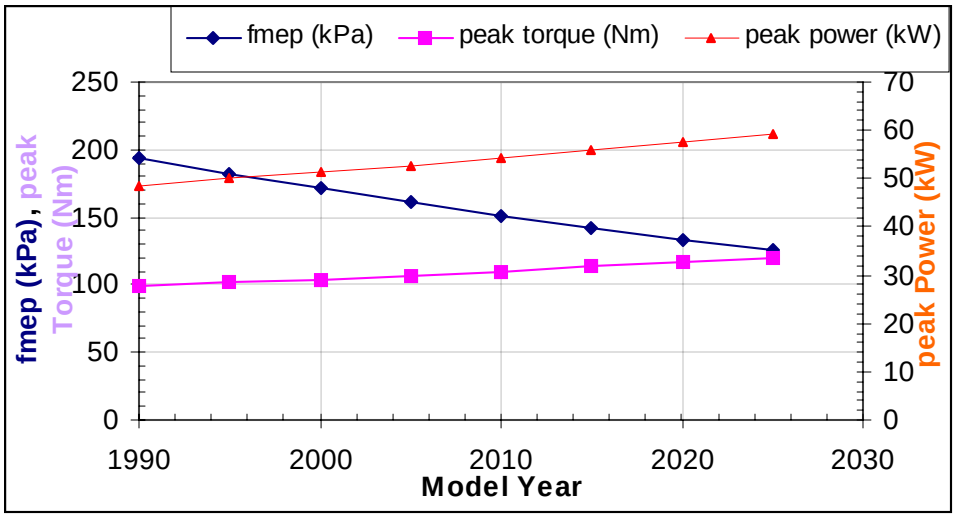

Figure 6. Projected gasoline engine trends over time [Chon & Heywood, 2000; Nam & Sorab, 2004].

Beyond incremental improvements in engine friction, it is difficult to predict how engines will change in the next 30 years. It is conceivable that production gasoline engines can have improved indicated efficiencies. This could be accomplished with the trend of "variable everything". The Atkinson cycle engine (as in the current Toyota Prius) is a good example of variable valve timing being used to increase efficiency at the cost of power. The lean burn engines of Honda (currently installed in the Civic HX, Hybrid, and Insight models) improve efficiency by burning gasoline under lean conditions at low loads.

The Honda Lean burn engine improves the best bsfc (best brake specific fuel consumption, or "sweet spot") over conventional engines by approximately 20%, and decreases friction by 8% [Ogawa, et al., 2003]. PERE models this with an indicated efficiency of ~0.48, with an 8% friction improvement. During higher engine speeds, the engine reverts to stoichiometric operation, where the engine is still more efficient than conventional engines (0.44). The engine speed breakpoint is not provided in the reference, so in PERE it is assumed to be 50% of the peak power rpm (6100 rpm*0.5).

There is less information on the Toyota Atkinson engine. PERE assumes that the efficiency is 15% greater than that of conventional engines, until the rpm cut point is reached [Heywood, 1988]. The peak torque values are decreased correspondingly. Beyond that point, it behaves as a conventional engine. This is similar to the lean burn engine.

Gasoline Direct Injection (GDI) or Homogeneously Charged Compression Ignition (HCCI) engines are also a promising alternative, though these are still mainly laboratory engines. In the near future, there may be engines with variable displacement, variable compression ratio, cylinder deactivation, etc. coming on to the scene. Moreover the current move toward 42 Volt power systems on the vehicle will allow for Integrated Starter Generator systems to start and stop the car during idle. This has been referred to as "minimal hybrid" in some references [An and Santini, 2004].

In addition to technical advances in engine design, it is possible that tire rolling resistance and vehicle aerodynamics can improve in the future. Currently passenger cars have tire rolling resistance of approximately 0.009. It is unlikely that these will improve significantly without sacrificing other performance measures. The aerodynamic resistance and vehicle frontal area of vehicles has room for improvement, but here, form tends to follow function, or design. Current cars have coefficients of drag approximately 0.30 - 0.35 (Toyota Camry $C_d = 0.30$). Vans and SUVs have Cd ~ 0.35 – 0.40 and pickups range from 0.40 – 0.45 [Gillespie, 1992]. The exceptional 2004 Toyota Prius has a C_d of 0.26, and the Honda Insight has the best in class coefficient of 0.25.

Hybrid Vehicles

Currently the most successful technology implemented commercially to improve the overall efficiency of vehicles is to hybridize their drivetrains, by adding an electric propulsion path to the wheels.

There are a number of electric hybrid vehicles on the road today: The Honda Insight was the first to be introduced in the United States in 1999. It was followed by the Toyota Prius and the Honda Civic (the Prius was first sold in Japan in 1997). Other manufacturers have also announced that they will release hybrid models of various kinds within the next few years.

There are several different kinds of hybrid vehicles under development. All share the common trait that there are two power sources that drive the vehicle forward during different operating modes. Most methods hybridize an internal combustion engine with an energy storage device such as a battery, ultracapacitor, or even hydraulic pump (fuel cell hybrids will be discussed in the next section). The hybrid configuration is usually either series or parallel. Series hybrids run off electric power only, and the batteries are recharged by the engine, which can run in an efficient mode. Series hybrids suffer from the disadvantage that both a large battery and motor are required, while losses are incurred in both charging and discharging the battery. Parallel hybrids run the drivetrain alternately with the engine, battery or both. This allows for a smaller battery/motor than the series hybrid and for the engine to run efficiently. The disadvantage compared to the series configuration is that the system requires more sophisticated strategy, packaging and transmission. Some models require a separate generator. The Honda hybrids are parallel, while the Toyota Prius is a combination series/parallel.

The spectrum of hybrids soon to be on the road is broad. General Motors is proposing a "minimal" hybrid version of its Sierra/Silverado truck, which is expected to improve fuel economy by 12%. By 2007, they announced a displacement on demand (cylinder deactivation) hybrid system for the Tahoe and Yukon line [GM, 2004]. Ford is set to release a full hybrid version of the Escape compact SUV in 2004. Honda announced that a hybrid version of the Accord will be sold in 2004, which will have Variable Cylinder Management (VCM) in its V6 engine [Honda, 2004]. Toyota announced the Highlander hybrid in 2005, while the Lexus 400 hybrid is expected in 2004 [Toyota, 2004]. All of the hybrids mentioned above are in (mostly) parallel configuration and store secondary energy in a battery. The Honda, Toyota, and GM

models also mainly use “advanced” gasoline engines. Many of the hybrids recharge the batteries by employing regenerative energy from the brakes.

With the promise of hybrids hitting many of the markets segments in the near future, it is imperative that any modeling of future vehicles include this class of vehicle. There have been a number of models developed, which captures the behavior of hybrid vehicles. ADVISOR (developed at NREL) is widely used in the research community [Kelly, 2001]. It models conventional as well as hybrid and fuel cell vehicles. ADVISOR is a relatively sophisticated model that can be run stand-alone or on the MATLAB® platform. Unfortunately, the model could not easily be integrated into MOVES for several reasons. Namely, the intensive data and effort required to calibrate the model is prohibitive for trying to model broad sections of the fleet required. It was thus necessary to adjust the approach so that a model could be run on the PERE spreadsheet. From there, it may either be run in spreadsheet mode, or programmed directly to link with MOVES in the future. The basic framework for PERE is similar to ADVISOR though: starting with a driving cycle input, calculate the road loads, then distribute the power and losses to the various energy conversion and storage media. Many other models exist as well, but the hybrid architecture in PERE is roughly based on the simple control logic described in Weiss et al., [2000] at MIT.

Strategy

Figure 7 shows the PERE flow chart for the parallel hybrid design. The battery can be any energy storage device (ultracapacitor or hydraulic). The logic control is relatively simple [Weiss et al., 2000]. When power demand is less than the hybrid threshold (2kW in the MIT case), the car runs on battery alone. Beyond the threshold, the car only runs on the gasoline engine. When power demand is greater than the peak engine power, then the battery assists or provides the needed boost. When braking, part of the energy is recaptured into the batteries. Each of the power paths described has its unique losses. This strategy is modified slightly in PERE to require that the hybrid threshold be set such that the state of charge on the battery is sustained over the course of the Federal Test Procedure driving cycle (city and highway), i.e. the battery ends the test with the same charge with which it started. Other differences in the approaches will be described below. The parallel power and state of charge algorithms are shown in Appendix A.

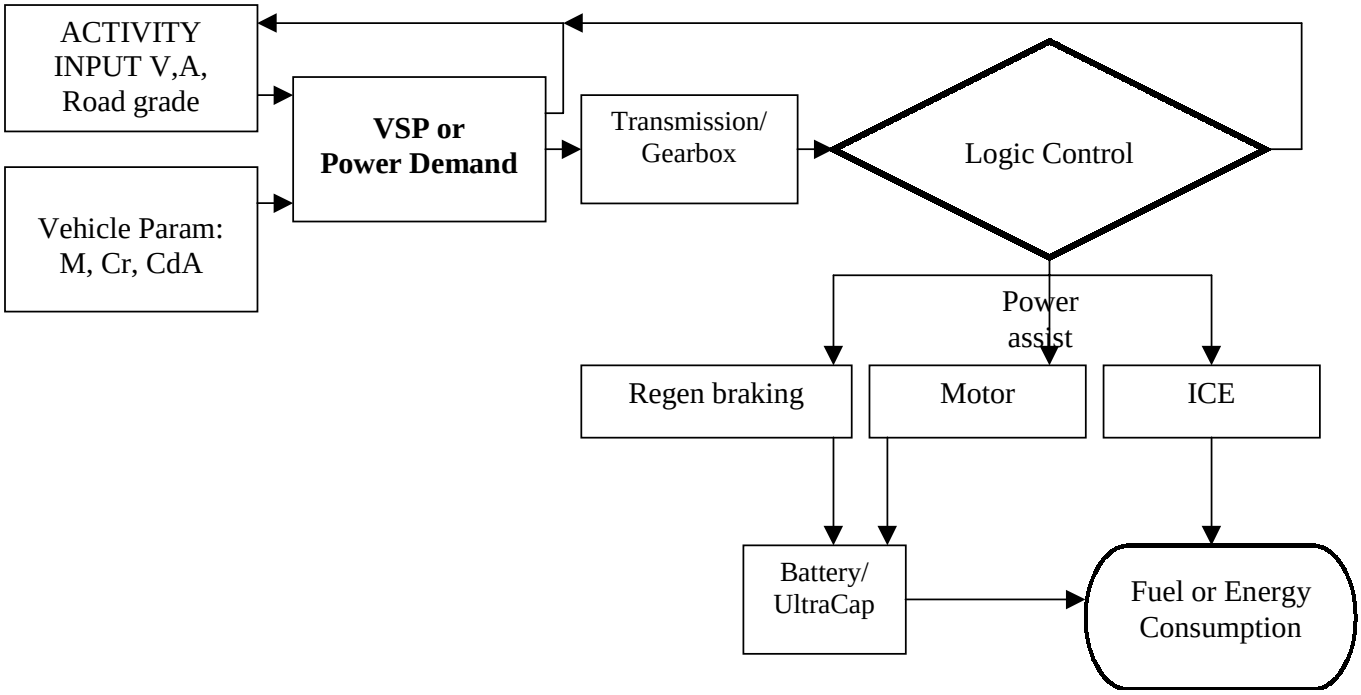

Figure 7. Parallel hybrid (gasoline/battery) flow chart.

Actual hybrid strategies can get much more sophisticated, where the battery can get recharged by the engine directly, during operation (as is the case for the Toyota Prius THS - Toyota, 2003). This system is a series/parallel architecture and is especially appropriate for stop and go driving. However, the PERE methodology takes the basic approach of distributing energy in the system defined by the strategy above, and taking into account losses. Thus, whether the energy is stored in the battery, or converted by the engine, the same overall energy is required, therefore the overall predicted fuel economy should be similar to what is measured (within 10%). The main omissions of PERE at this time is that it does not include a cold-start module. Cold start factors will be inserted by MOVES, not PERE. Hybrid vehicle fuel consumption can be significantly larger during cold start to heat the catalyst to light-off temperatures and also to charge up the batteries or capacitors (if needed). Cold start factors are discussed in greater detail in the Sensitivity section.

Hybrid threshold was chosen in order to give close to net zero state of charge over the FTP and HWY driving cycles. More explicitly, this usually means that the battery discharges during city type driving, and recharges during highway type driving. This loosely simulates a “charge sustaining” strategy (‘pseudo-charge sustaining strategy’). For all the hybrids modeled in this report, this threshold fell between 2 and 4 kW. Values are in Appendix B. This strategy implies that the batteries are only being recharged through regenerative braking, and not the engine.

Motor/Generator/Inverter

The conversion between electrical and mechanical energy is done with a motor. In reverse this is called a generator. For hybrids, we will use the term “motor” to indicate both devices. In PERE the motor operates both forwards and backwards at different times depending on the driving,

with different losses. Weiss et al. [2000] estimates the motor system efficiency to be 76% with an additional 15% loss during regenerative braking. The motor efficiency (alone) is likely higher, approaching 90% for a permanent magnet brushless DC motor, though it depends on the size of the motor [Laramie and Dicks, p. 279 2000, Ogawa, et al., 2003]. However, the MIT value includes other system losses (such as from an inverter, which can have efficiencies of ~94%). Moreover, motor efficiency depends somewhat on the operating mode, but PERE also assumes a fixed value for simplicity.

The motor power and torque curve is shown in Figure 8. It is scalable with peak power [Weiss et al., 2000]. The motor in the model is connected to the transmission, not directly to the wheels (except in the fuel cell).

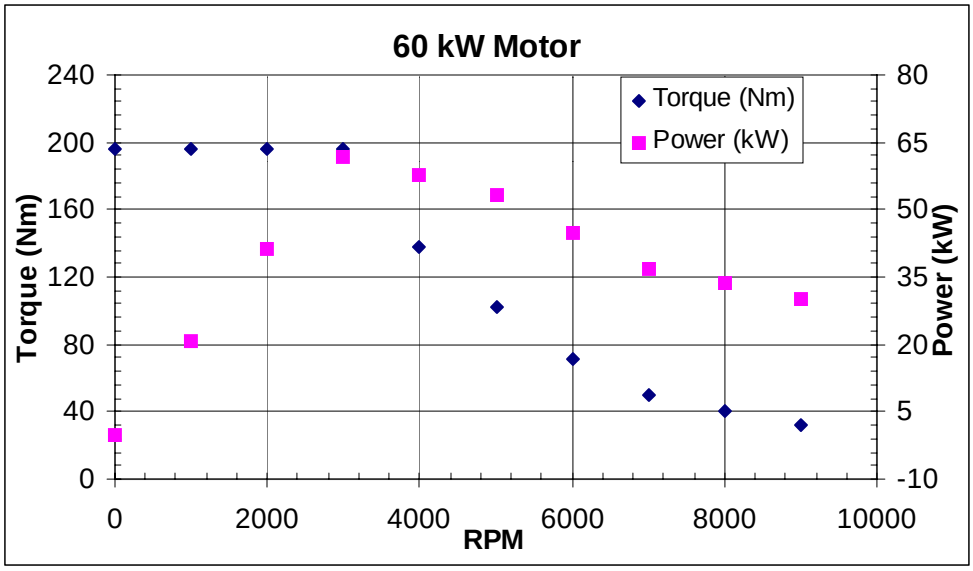

Figure 8. Motor peak torque and power from Weiss et al. [2000].

For the sake of nomenclature, we define the terms “mild” and “full” hybrid. There is no standard definition in the literature since there are no clear demarcations, only a continuous spectrum of possibilities. In one reference, the separating value is defined by the ratio of peak motor power to peak motor + engine power [An and Santini, 2004]. So a convention vehicle powered with an engine has a ratio of 0, and a “pure” battery electric vehicle has a ratio of 1. This report remains consistent with this approach and defines mild hybrid as having a ratio < 0.25. An example is the Honda Civic Hybrid (~0.14). The full hybrid has a ratio =>0.25. The 2004 Toyota Prius has a rating of ~ 0.47. This definition does not necessarily imply that mild hybrids are worse, or less efficient than full hybrids. In reality, however, the size of the motor is meaningless without a battery (or ultracapacitor) that can manage the current flows in and out of it. The effect of hybridization naturally depends on the hardware, and what functions are built in, moreso than the ratio of any two numbers.

Energy Storage Devices – Batteries, Ultracapacitors and Hydraulics

Batteries on hybrid vehicles tend to be of the nickel metal hydride (NiMH) variety. They have relatively high energy densities and can withstand many charge/discharge cycles, while being affordable. Compared to a conventional vehicle, however, batteries add significant cost.

In PERE, each second the power draw (discharge) from the battery is adjusted by the discharge efficiency (95%) as well as the motor efficiency. To be more accurate, this efficiency really depends on the state of charge of the battery, but we will approximate it as constant. During brake recharge, the rate includes a regenerative brake efficiency of 85% [Weiss et al., 2000]. There is added loss due to fact that front wheel drive hybrids only can recapture braking power from the front wheels (not the rear). Thus up to approximately 75% of the braking energy is available for recapture [An and Santini, 2004]. However, the new Prius brake by wire system can recapture significantly more [Toyota, 2003]. After the losses are included, the power is integrated over each second of the driving cycle, and then the discharge (positive) and recharge (negative) totals are added to give a final state of charge (SOC), as a fraction of the kWhr rating. The final state of charge over the FTP driving cycle is calibrated to be close to zero in our model. Unfortunately, it may not be true for other driving cycles. A more sophisticated charge sustaining strategy is a possibility for future version of PERE.

The battery is assumed to have a rating of 0.936 kWhr on the mild hybrid, the nominal rating for the Honda Insight (the Civic is 0.864). For the full hybrid, the battery is assumed to be similar to the ’04 Prius, or 1.31kWhr. However, because we have a ‘pseudo-charge sustaining strategy’ and the vehicle is not assumed to drive on any extremely aggressive driving cycles, this number does not affect the model. In reality it is more important to define the limitations of the hybrid based on the total electrical power generated from the battery/motor system. PERE simplifies this, by placing emphasis on the motor system only. This assumes that manufacturers will integrate a “properly” sized battery for the motor. If PERE is required for high performance (0-60mph) runs, this, and other, portions of the model may require revision.

Replacing a battery with an ultracapacitor changes the model slightly. The discharge and recharge efficiencies would be different, as would its ability to recapture energy from higher power braking events.

Hydraulic hybrids combine internal combustion engines with an hydraulic energy storage device. This storage device stores the energy in pressurized gases. The hydraulics would respond similar to an ultracapacitor except that the link would be mechanical, rather than electrical. This would increase recapture efficiency. The EPA is developing this technology with industry partners through cooperative research and development agreements, including implementation of the technology on a number of prototype vehicles [Alson et al., 2004].

Options for including hydraulic and ultracapacitor hybrids in MOVES are to model these different energy storage devices as separate engine technologies (source bins), using PERE or existing fuel consumption rates on these technologies [e.g. Alson et al., 2004]; or, to create a “generic hybrid” engine technology and modify the hybrid component of PERE to account for hybrids with battery, hydraulic, or ultracapacitor storage devices. These options are currently under consideration.

Vehicle Weight and other Specifications

Hybrid vehicles are usually able to downsize the engine in order to save weight and fuel further, however the added components of the motor, inverter, battery, and other connecting components more than compensate for the engine weight loss. Previous studies have summed the weights of the components based on power density in order to estimate a vehicle weight. This method has limitations in that other structural and component weights may be omitted. This report uses a different approach. The weights of existing hybrids are compared with their conventional vehicle counterparts. Table 2 shows the weights of various hybrid vehicles. In particular the Honda Civic Hybrid is compared with the Civic DX, and the Dodge Durango hybrid is compared with the Durango 4WD. While the Durango is no longer planned for production, it is still useful to compare specifications. The Prius and Insight obviously have no direct partner, so no direct weight comparison could be done. The weight ratio of hybrid to non-hybrid is found to be 1.07, or a 7% increase. This is based on the ratio of test weights, which is curb weight + 300 lbs. The diesel hybrid is assumed to have a 4% increase over its gasoline hybrid counterpart. As more hybrid versions of vehicles are released, this mass increase ratio estimate can be improved.

Table 2: Hybrid Vehicle Specification in Comparison to Conventional (if exists). All sources are from Manufacturer, Car&Driver or Road&Track websites.

	model	max torque	max power	displacement (l)	curb weight (kg)	Motor Power	Battery Capacity (kWhr)
Hybrid	**Honda Insight**	89.5N-m@ 2000rpm	50kW@ 5700rpm	0.995	853	10.4kW@ 3000rpm	0.936
	Honda Civic Hybrid	118Nm@ 43300rpm	63.4kW@ 5700rpm	1.339	1213	10.kW@ 3000rpm	0.864
	2003 Toyota Prius	111N-m@ 4200rpm	52kW@ 4500rpm	1.497	1254	33kW@ 1540rpm	1.31
	2004 Toyota Prius	111Nm@ 4200rpm	57kW@ 5000rpm	1.497	1311	50kW@ 1540rpm	1.31
	Dodge Durango	305N-m	130.6kW	3.9	2389	66.4kW	?
Conventional	**Honda Civic DX**	149Nm@ 4500rpm	86kW@ 6100rpm	1.668	1111		
	Honda Civic HX	151Nm@ 4500rpm	87.3kW@ 6100rpm	1.668	1111		
	Toyota Camry SE	220Nm@ 4000rpm	117kW@ 5600rpm	2.4	1425		
	Dodge Durango 4wd	475Nm@ 3000rpm	186kW@ 4200rpm	5.9	2251		

Many of the other vehicle attributes that aren't published had to be approximated. Often coefficients of drag and weights are available, but rolling resistance is not. Frontal area is approximated from the published dimensions (Equation 2) if a direct measurement is not provided.

The table of hybrid coefficients are also in Appendix B. Many of the variables may have a model year relationship into the future. E.g. component weights, Cr, Cd, Pacc, motor efficiency, regeneration braking efficiency, discharge/recharge efficiency, etc. However, most of these are expected to drop somewhat and level off in the near future. The accessory term (Pacc) is the only

term expected to rise in the next few years with the addition of more electrical loads (and luxuries).

Accessories

Currently, PERE does not model air conditioning or heat in hybrid (or fuel cell vehicles). Therefore the accessory loads are a relatively small portion of the power required (~0.75 kW). However it is not insignificant, if the accessories were run completely on the batteries, there would be less power remaining for accelerations. In addition it is expected that accessory power will increase in the future.

In PERE, the accessories are run off the battery when the battery is on a discharge cycle. Otherwise it runs off the generator (engine). The algorithms are listed in the Appendix A.

Air conditioning and heating are potentially large loads for hybrid vehicles. From a fuel economy reference, the accessory loading can be large. In MOVES, the effect of air conditioning will be applied to the base AC-off energy consumption rates developed by PERE.

Model Calibration

Since the PERE hybrid strategy model is based on Weiss, et al. [2000], the model is 'calibrated' to the model "MIT hybrid" vehicle. The MIT report gives most of the vehicle parameters required for the model. Figure 9 compares the fuel economy results of PERE with the MIT hybrid. Figure 10 compares the state of charge of the batteries following the FTP test. Since the models are not identical, differences are expected. However, the fuel economies are an excellent match. This indicates that the modeling methodologies are quite similar.

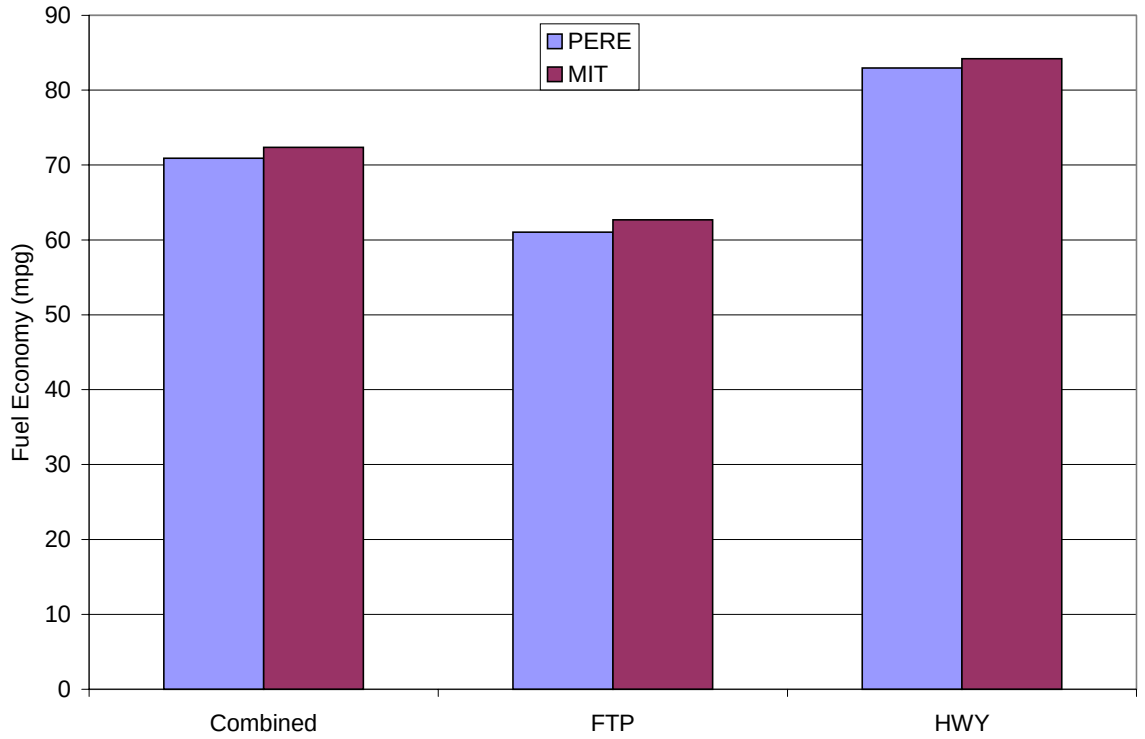

Figure 9. Fuel economy of a model year 2020 hybrid car compared to MIT study [Weiss et al., 2000].

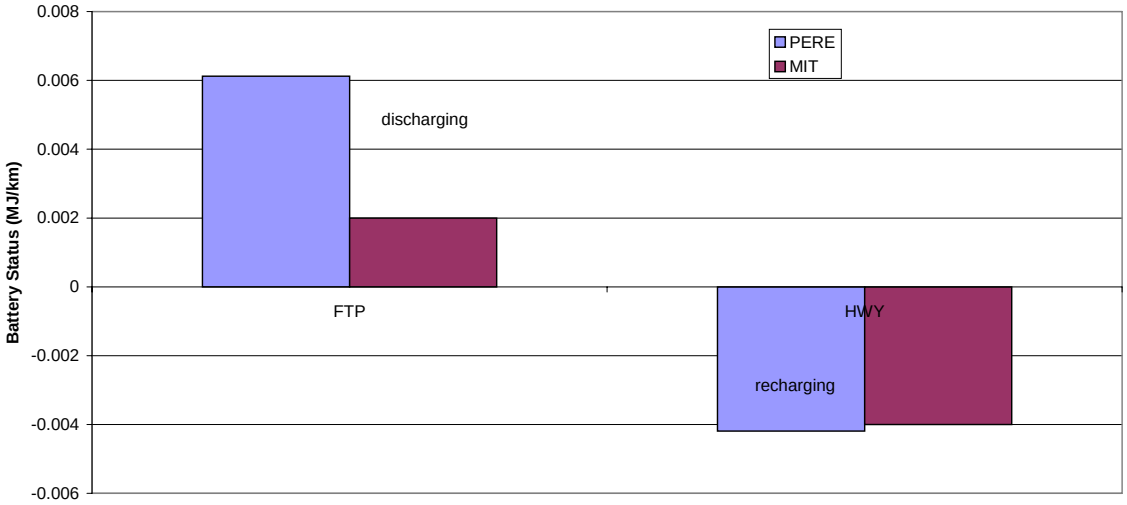

Figure 10. State of Battery compared to MIT study [2000].

The differences b/w MIT and PERE models are listed below:
1- PERE does not include bag 1 cold start. The MIT report does not mention if cold start effects are included in their model.
2- MIT transmission model is unknown. (minor effect)
3- Hybrid threshold is determined differently
4- Battery recharge model probably is not identical.
5- PERE adds additional loss from front wheel drive regenerative braking only.
6- Engine friction model is slightly different.

Validation Results

It is difficult to conduct validation results with real hybrid vehicles, when the model is only an approximation of a hybrid vehicle. Actual hybrid vehicles have much more sophisticated control strategies, as well as efficiencies that depend on various operating conditions. However, the energy flows still follow a similar physical and logical progression. Given a power demand the fuel consumption rate should be similar if the loss terms are characterized sufficiently well.

The validation is conducted on a number of vehicles (hybrid and non-hybrid), whose specifications could be found on either the manfuacturer's, or a trade magazine website (such as Car and Driver and Road and Track). All weights are test weights (curb weight plus 300lbs). The list of vehicles is on Table 3. The Honda Civic HX is the lean burn engine version of the Civic series.

Table 3. Validation vehicles – all model years are 2004 unless otherwise specified.

Mfr	Model
Toyota	Camry
VW	Jetta gas
VW	Jetta Diesel
Honda	Civic DX
Honda	Civic HX
Honda	Civic Hybrid
Honda	Insight
Toyota	Prius '01
Toyota	Prius '04

The validations are conducted in comparison to unadjusted EPA certification fuel economy numbers. The rated fuel economy numbers for production vehicles are adjusted based on real world driving correction factors: adjusted FTP = unadjusted FTP*0.9 and adjusted HWY = unadjusted HWY*0.78. PERE's output should be compared with the dynamometer measured fuel economy, which are the unadjusted numbers, since PERE is modeling the physical loads on the vehicle as imposed by the dynamometer directly. The combined fuel economy (miles per gallon) is a weighted average 0.45 (FTP) and 0.55 (HWY), calculated in the following standard fashion [Schaefer, 1994]:

$$\text{Combined F.E.} = 1/(0.55/\text{FTP} + 0.45/\text{HWY}). \quad (12)$$

Figures 11, 12, and 13 show the validations for the vehicles (city, highway and combined respectively). The model performs especially well for conventional vehicles. There were several other conventional vehicles (light cars and trucks) validated, the Camry, Civic, and Jetta are the only ones shown. All of the conventional vehicles matched rated fuel economy to within 5% (on city and highway) with the exception of the Volkswagon Jetta (gasoline). There were also several conventional vehicles validated to dynamometer tests in previous studies, using a similar, but older version of PERE [Nam, 2003]. Although the Jetta (1.9L TDI) results were within 5%, the reason for the discrepancy with the Jetta (gas) is unknown. For a small fraction of vehicles, the fuel economy is not accurately captured by PERE. This is most likely due to many different factors unique to each make and model. It is also interesting to note that PERE slightly overestimates fuel economy from the city for many of the vehicles. This is not too surprising since cold start factors are not included.

The "advanced vehicle" validations begin with the Honda Civic HX, with the lean burn engine. The predictions for this vehicle is very good (within 5%). This suggests that the powertrain model is correctly modeled, based on the description of the lean burn engine by Ogawa et al. [2003]. All of the advanced vehicles are accurately capture by PERE for highway driving (within 5%). With the exception of the Toyota Prius, the city estimates are also all within 10%. PERE overpredicts the fuel economy on the Honda Hybrid on the city cycle by around 9%. This is likely due, in part, to the lack of a cold start module in the present version of PERE. Hybrids are especially expected to have significantly higher fuel consumption during the cold start first phase (bag 1) of the FTP. This is due to the fact that the engine has to stay on in order to ensure that the catalyst lights off in a timely fashion (after which it can start breaking down the criteria pollutants). Many conventional engines also run slightly rich during the start up period. Presently PERE shuts the engine down during decelerations and idle, which would tend to significantly

under predict fuel consumption (over predict fuel economy) during start-up for hybrids, and to a lesser extent conventional engines. Changing PERE so that the engine remains on for the first two minutes would be relatively simple. Despite this, PERE still underpredicts city fuel economy for the Prius by 12% and 18% for the 2001 and 2004 models respectively. This demonstrates how different the strategy of the Prius is from the rudimentary strategy employed in PERE. The Toyota Hybrid System (THS) is a series/parallel hybrid design. A powersplit device routes some of the power from the engine to recharge the batteries, thus the motor is used much more frequently than in parallel hybrid [Toyota, 2003] to supplement power. The hybrid system can be fine-tuned to give optimal fuel economy. The brake-by-wire system on the 2004 Prius also helps to regain maximal energy from regenerative braking. In this way, the Prius can and does get better fuel economy in the city than on the highway (a difficult condition for PERE to duplicate). Moreover, the specifications (efficiency improvements) for the Prius Atkinson cycle engine are unknown.

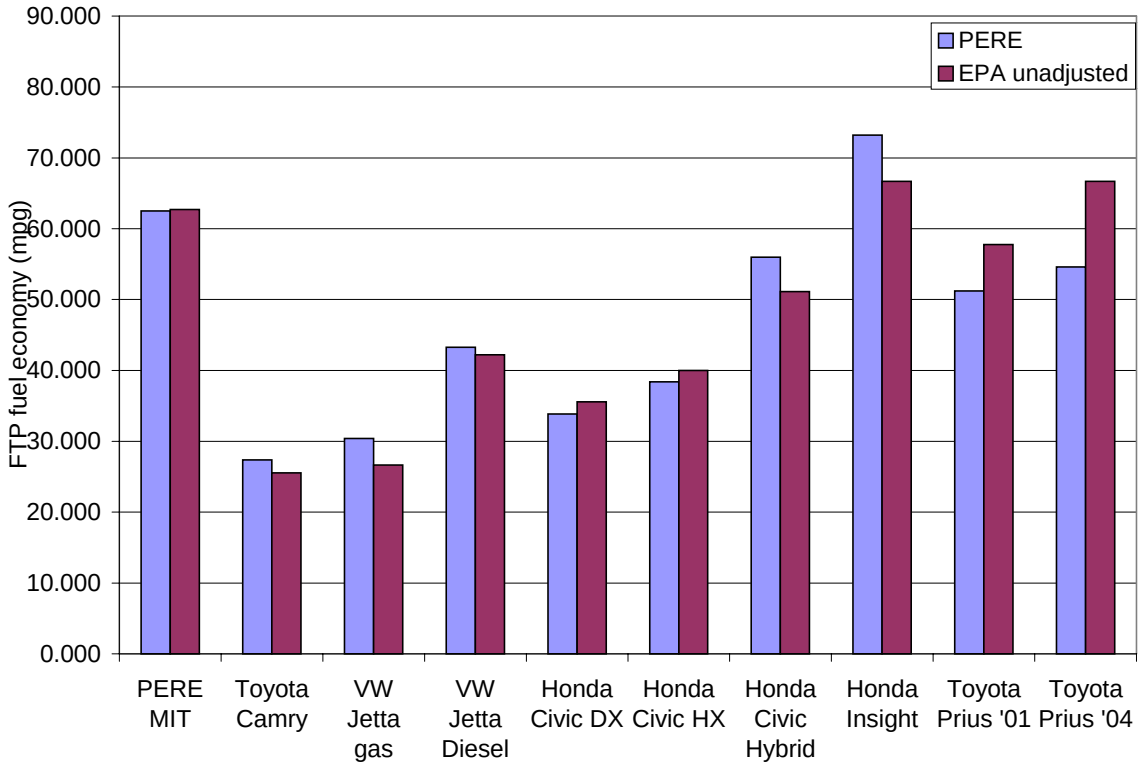

Figure 11. Fuel Economy validation for the FTP city (UDDS) compared to unadjusted EPA figures.

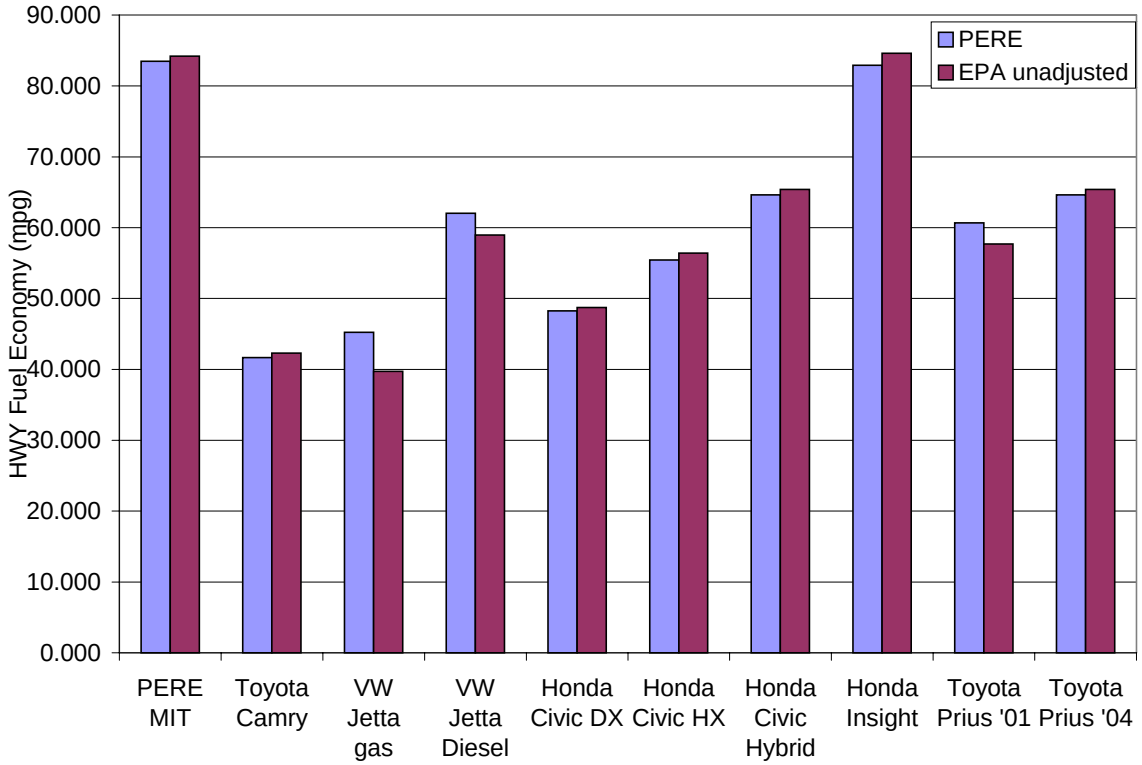

Figure 12. Fuel Economy validation for the FTP (HWY) compared to unadjusted EPA figures.

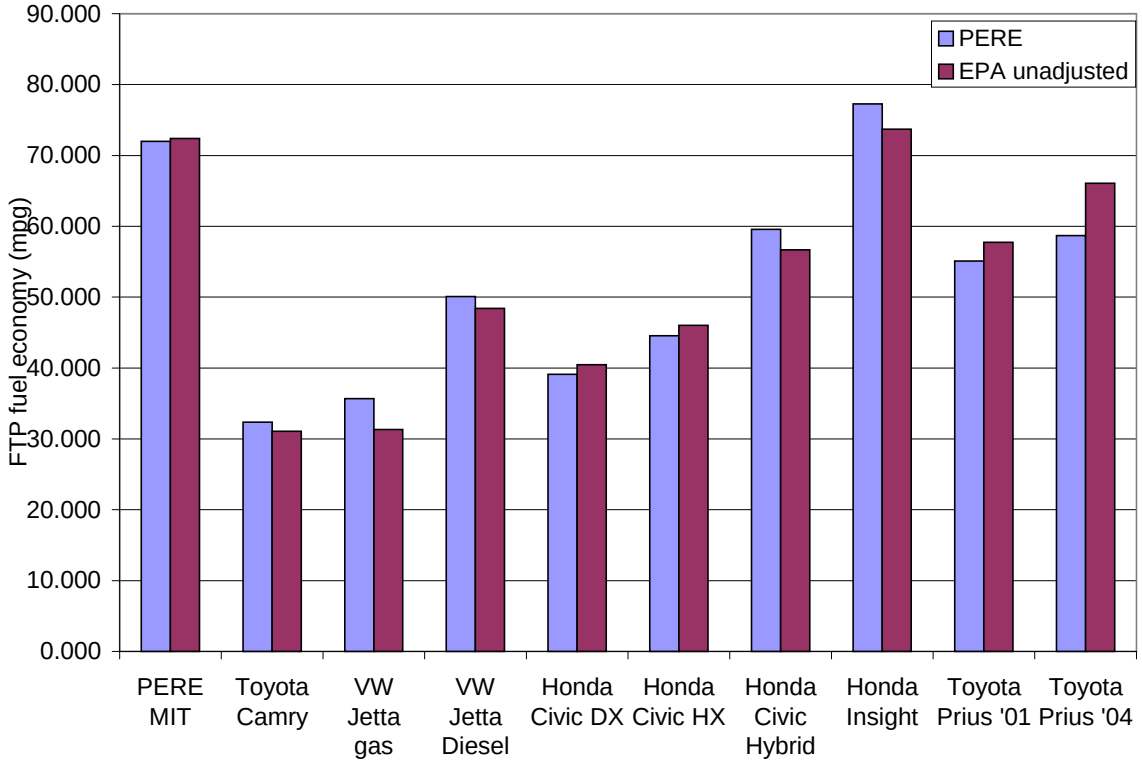

Figure 13. Fuel Economy validation for the FTP/HWY Combined compared to unadjusted EPA figures.

It has been demonstrated that PERE can capture the fuel consumption behavior of gasoline, diesel, and "generic" parallel hybrid vehicles. The vehicle parameters required from the user are model year, weight, body type (size, which can be approximated), engine displacement, motor power, and fuel type. With the exception of body type, these are the primary "source" inputs for MOVES.

This simplification of hybrid control strategy modeling could result in under-predicting fuel economy. A more optimized control strategy would be to run the battery at low load and allow the engine to recharge the battery at higher loads, where the engine can operate more efficiently (as the Prius does). This was not done because it was difficult to put in spreadsheet format. If PERE is coded, then a more sophisticated control algorithm could be added.

Fuel Cell Vehicles

While, there are several types of fuel cells, the hydrogen Proton Exchange Membrane (PEM) fuel cell is the fuel cell of choice for vehicle applications. A fuel cell is a power source that runs on hydrogen to make current across a Proton Exchange Membrane. Each cell produces a small amount of current and (like a battery) these are stacked together to produce a relatively efficient power pack. There are other types of fuel cells, but PEM cells are the most commonly researched today. Most prototype vehicles are equipped with Hydrogen PEM stack fuel cells. Hydrogen is the primary energy source, which produces energy when combined with oxygen. This reaction produces water, which is the only tailpipe emissions. Some fuel cell systems use a reformer to break hydrocarbons from liquid fuels into gaseous hydrogen, but this technology appears to be falling out of favor for light duty vehicle use due to its size and relative inefficiency.

In PERE, fuel cell vehicles are modeled as "series hybrid" vehicles. This means that there is only one mechanical path. However, there is still a parallel electrical power path, in that either the battery or fuel cell can drive the motor. This model is similar to the one proposed by Weiss et al. [2000 & revised in 2003] (there is still a hybrid threshold required). The power flow chart is shown on Figure 14. It is essentially the same as the hybrid model above, but the engine is replaced with a fuel cell, and there is no transmission (only a single gear driven by the high speed motor). The fuel cell system efficiency (from the same reference) is shown on Figure 15. The fuel cell efficiency curve is a projection and reflects an optimistic estimate. The figure shows the efficiency points (scaled to a 72 kW cell) including a 7^{th} order polynomial fit for PERE. The fit allows for ease of interpolation in a spreadsheet.

Again in this version of PERE, there is no cold start modeled, the effects of which can be significant. We also use the battery, similar to a parallel hybrid, to 'launch' the vehicle below the hybrid threshold (initial acceleration). This avoids the very low fuel cell system efficiencies at low load (see Figure 15). The model is similar in structure to the hybrid presented above. The "calibration" comparison to the MIT results is shown in Figure 16. The fuel economy figures are calculated in miles per gallon gasoline equivalent by converting the work equivalent hydrogen into gasoline mass (with their respective lower heating values). This vehicle is found to have a tank to wheel efficiency of 50%. The tank to wheel efficiency is simply defined here as the

useful energy out/fuel energy in. The useful energy out is only the (positive) energy required for the car to follow the driving cycle. It would be slightly lower if the accessories were included.

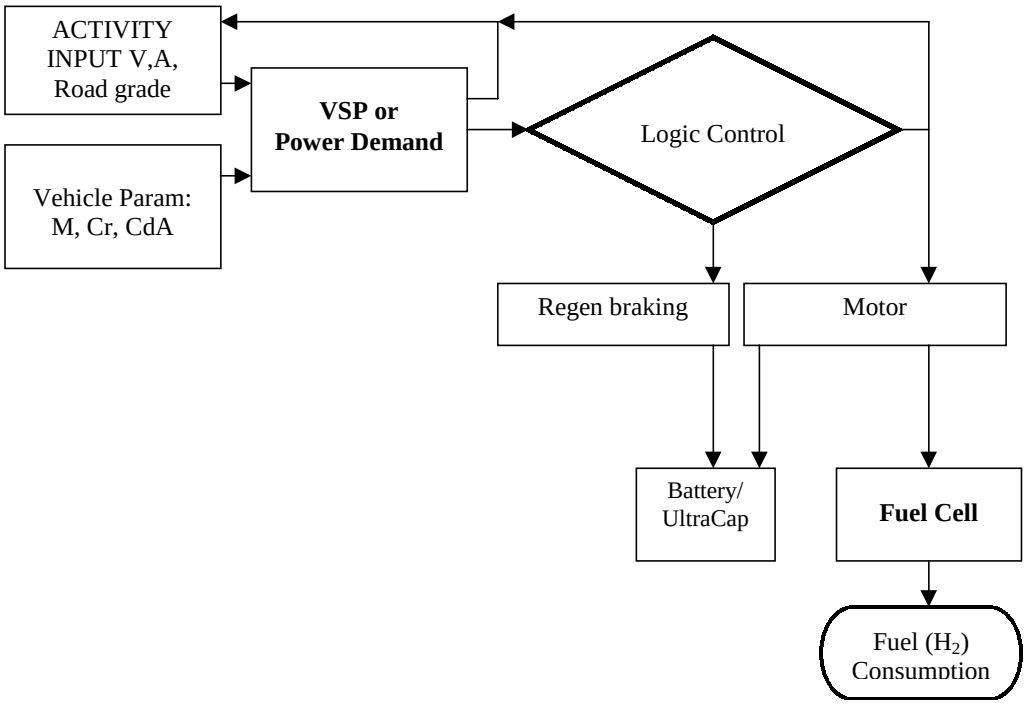

Figure 14. Power flow chart for the hydrogen hybrid fuel cell vehicle.

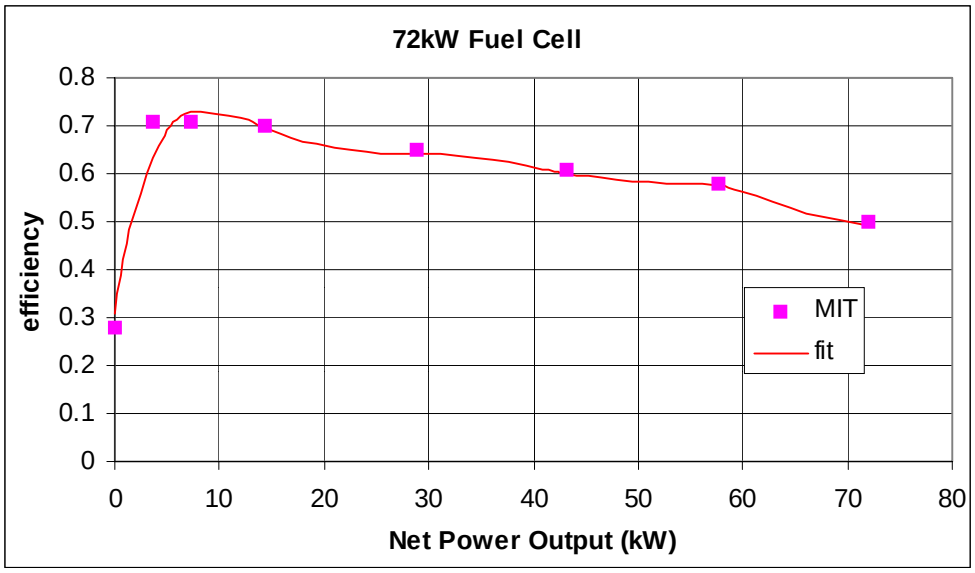

Figure 15. Fuel cell integrated system efficiency [Weiss et al, 2000, 2003] including a 7th order polynomial fit.

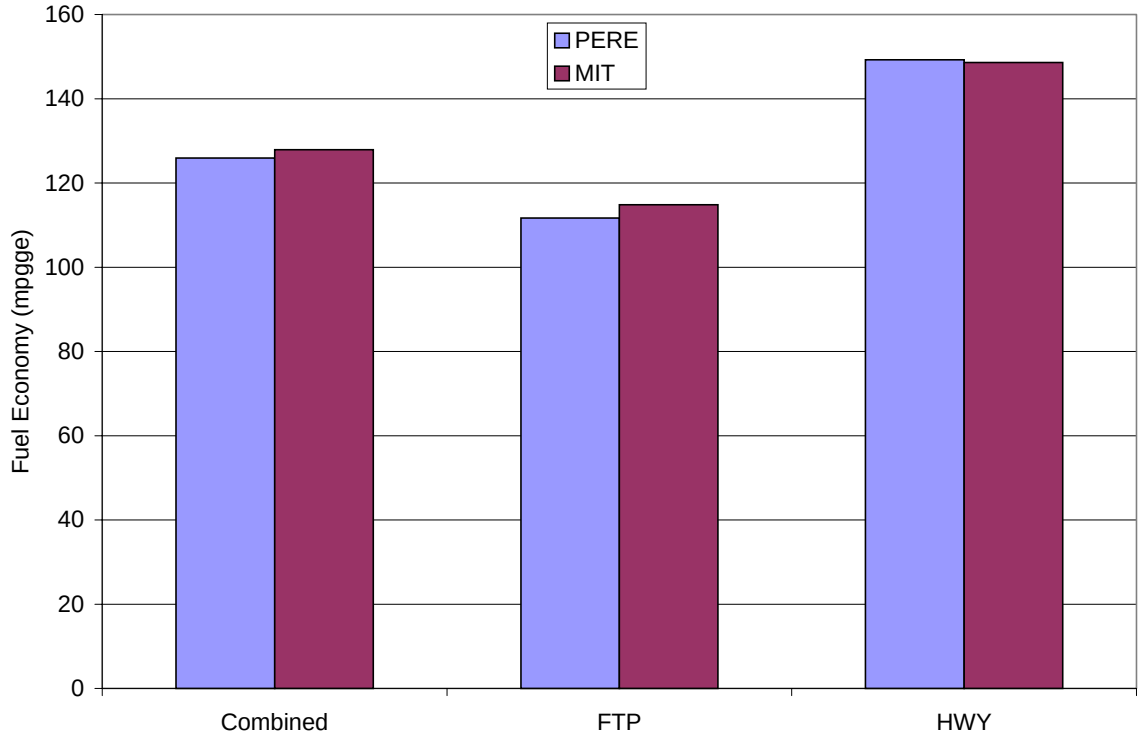

Figure 16. Fuel economy comparison between PERE and Weiss et al [2003]. The units are in miles per gallon gasoline equivalent.

Validation

It is difficult to conduct a validation of the fuel cell model since there isn't a tremendous amount of data available for the prototype vehicles that exist. Some specifications have been collected for a number of manufacturer prototypes. They are listed on Table 4 along with the conventional vehicle body on which the vehicle is built (the Daimler Chrysler F-Cell vehicle weight is unknown). The Honda FCX has a unique body, so it does not have a conventional vehicle equivalent (though it does have a similar electric vehicle). The average increase in weight of the first 3 vehicles compared to its equivalent conventional vehicle is 23%. This increase is expected to be less for larger (medium and heavy duty) vehicles.

Table 4. List of some fuel cell vehicles. (References are all from information sheets distributed during ride&drives by manufacturer representatives, or from website)

	model	Eng power (kW)	curb weight (kg)	Motor Power (kW)	FC power (kW)
Fuel Cell	Ford Focus		1600	65	80
	Toyota FCHV		1860	80	90
	GM Hydro-Gen3		1700	60	94
	DC FCELL		N/A	65	80
	Honda FCX		1684	60	80
Conventional	Ford Focus	97	1213		
	Toyota Highlander	119	1597		
	GM Opel Zafira	74	1393		
	DC Mercedes A-Class	76	1115		

The Ford, DaimlerChrysler, and Honda vehicles all use the Ballard® Mark 902 fuel cell stack. The GM Hydrogen 3 and Toyota FCHV use different stacks. The former is not an hybrid. As the fuel cell energy densities increase in the future, the weight increase is expected to be reduced from the current estimate of 23%. The estimated system efficiency for the 80kW fuel cell is different from the one on Figure 15 (which can be used for future projections). The more conservative estimates are shown on Figure 17. These are used for the validations below.

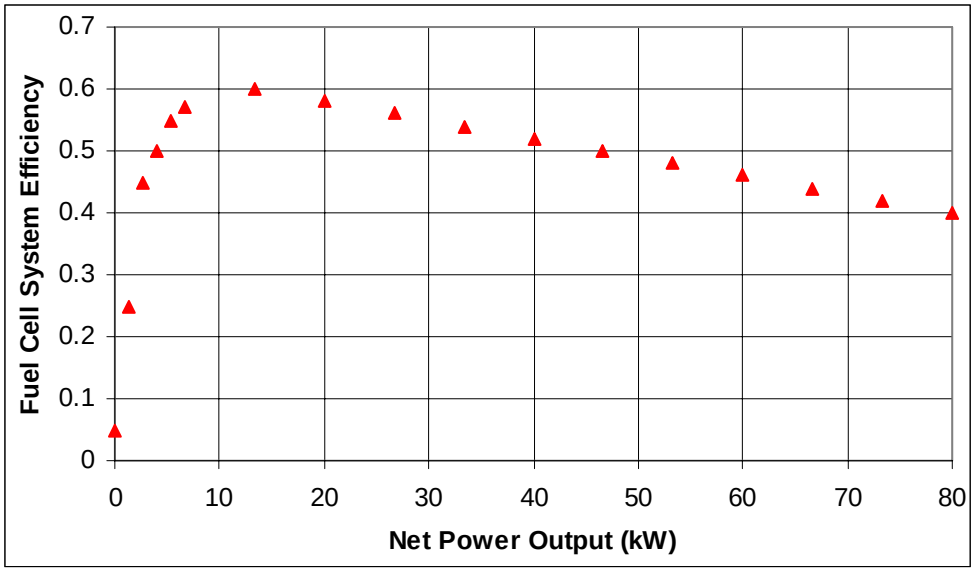

Figure 17. Fuel Cell System efficiency for an 80kW stack [Nelson, 2003].

Validations can only be conducted on the Honda FCX, since this is the only vehicle whose fuel economy equivalent numbers are known.

In order to model the Honda FCX, some of the energy storage parameters had to be adjusted since the vehicle is equipped with an ultracapacitor, rather than a battery and does not have a DC-DC converter. The motor system, and recharge efficiencies are higher. The Honda FCX has an adjusted EPA fuel economy rating of 51/46 miles per kilogram hydrogen (city/highway). A kg of hydrogen is roughly equal to a gallon of gasoline in energy. In comparison, PERE's predictions are shown on Figure 18. The discrepancy is within 5%.

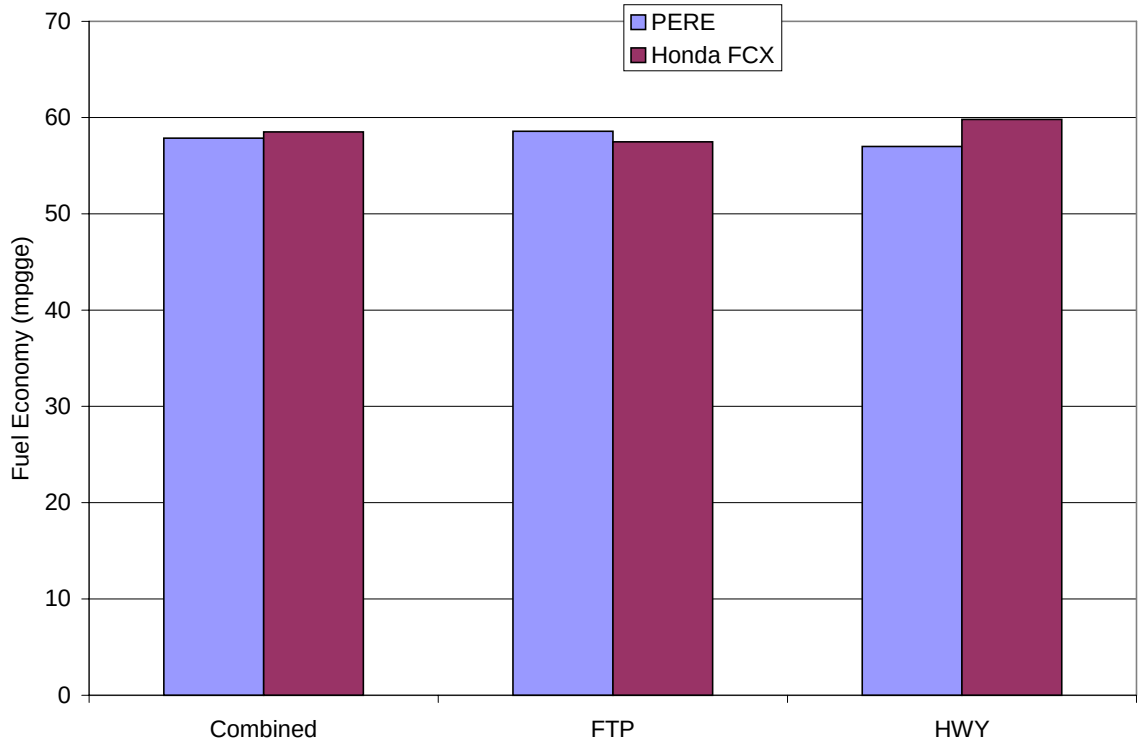

Figure 18. Fuel economy (in miles per gallon gasoline equivalent) for the Honda FCX.

Sensitivity

This section is devoted to a sensitivity analysis of PERE. The analysis determines which parameters are most important to characterize accurately. A static sensitivity is performed in relation to a change in city vs highway fuel consumption. It is necessary to do a separate analysis since the parameters affect the results from two different driving types in a disparate fashion. The simple static sensitivity test assumes a 10% variation in each parameter (though some of the parameters are correlated). The change in the fuel consumption result is ranked and compared. In order to perform a more complete uncertainty analysis, it is necessary to quantify the variation in the parameters. This is a potentially difficult undertaking, since some of the parameters are estimates (and not measurements). However, a more complete analysis will be performed in a future report.

Table 5 shows the sensitivity results, in % difference, for a typical modern passenger car modeled using PERE. To get the relative sensitivity, divide by 10. TRLHP is the Track Road Load Horsepower. It is a single quantity on which the (track) road load coefficients (A,B,C) are based in MOVES. PERE does not typically use TRLHP, but MOVES does. As expected, the parameters most affecting fuel consumption tend to be different for city vs highway driving. It is not surprising though, that the efficiency, weight, and engine displacement all dominate the top ranking. Fortunately, these quantities are typically known inputs for the model, or in the case of indicated efficiency, should not vary much. For those advanced engines where the efficiency is unknown, it clearly poses a problem for the model. The high ranking of the transmission efficiency might support the need for a speed or load based transmissions model. Aside from efficiency and N/v, however, PERE seems to be relatively insensitive to the other transmission parameters. However, it is important to make sure that the gear ratios are not systematically off from the actual gear ratios. It is interesting also to note that the model is quite insensitive the peak torque curves. It would be more crucial if high acceleration (full throttle) performance modeling was being performed. Since the activity in MOVES describes representative "real-world" driving, these driving modes are not stressed in the model, nor is it in PERE. Though it is not included the table, the model was not sensitive (<1%) to the rotational term in Equation 1 (ε).

Table 5. Static sensitivity test for the PERE parameters used to model a typical conventional passenger car. Parameters are adjusted 10%.

RANK	Parameter	Error City
1	P/T indicated eff (eta)	4.93
2	Engine Displ (L)	4.57
3	trans eff	4.46
4	Vehicle wgt (kg)	3.98
5	k0 (N indep friction kJ/l	3.72
6	N/v (rpm/mph)	3.31
7	TRLHP	1.95
8	Shift point 3-4	1.31
9	g/gtop 4	1.26
10	Shift point 2-3	1.24
11	Shift point 4-5	1.11
12	Cr0 (rolling resistance)	1.05
13	g/gtop 5	0.96
14	Cd (drag coeff)	0.93
15	A (frontal area m^2)	0.93
16	Nidle (rpm)	0.90
17	k1 (N dependent fric)	0.85
18	Pacc (accessory - kW)	0.52
19	g/gtop 1	0.38
20	g/gtop 2	0.22
21	g/gtop 3	0.16
22	Shift point 1-2 (mph)	0.04
23	torque curve up 10%	0.03

RANK	Parameter	Error Hwy
1	P/T indicated eff (eta)	5.92
2	trans eff	5.55
3	TRLHP	5.14
4	Engine Displ (L)	3.49
5	Cd (drag coeff)	3.11
6	A (frontal area m^2)	3.11
7	Vehicle wgt (kg)	3.01
8	k0 (N indep friction kJ/l	2.75
9	Nidle (rpm)	2.27
10	g/gtop 2	2.25
11	g/gtop 1	2.25
12	Shift point 2-3	2.22
13	Shift point 1-2 (mph)	2.21
14	N/v (rpm/mph)	1.89
15	g/gtop 3	1.88
16	Cr0 (rolling resistance)	1.88
17	Shift point 4-5	1.46
18	Shift point 3-4	0.91
19	k1 (N dependent fric)	0.74
20	g/gtop 4	0.67
21	Pacc (accessory - kW)	0.40
22	g/gtop 5	0.23
23	torque curve up 10%	0.00

The sensitivity results for a "typical" full hybrid are presented in Table 6. Here the motor is power split such that it can bypass the transmission. This improves the efficiency of the vehicle. This is a fictional hybrid vehicle designed using PERE only, but assuming the same body and

overall power as the previous vehicle. The transmission parameters have been omitted from this analysis. The hybrid threshold was adjusted to maintain the pseudo-charge sustaining strategy with each run. It is clear from this table that the engine parameters are still more important for fuel economy modeling compared to the electric parameters. Since the small engine is operating at much higher loads, the model is much more sensitive to changes than the conventional vehicle. Again, since the vehicle is able to meet the drive cycle (sometimes with the help of the motor), the battery limit parameters are not important for the model.

Table 6. Static sensitivity test for the PERE parameters used to model a fictional full electric hybrid passenger car.

RANK	Parameter	Error City
1	P/T indicated eff (eta)	8.11
2	Vehicle wgt (kg)	7.18
3	Engine Displ (L)	5.42
4	overall motor efficiency	3.38
5	Cr0 (rolling resistance)	3.32
6	Cd (drag coeff)	3.12
7	A (frontal area m^2)	3.12
8	torq curve up 10%	2.96
9	Regen Brake Eff	1.99
10	FWD power frac	1.99
11	Motor peak power (kW)	1.08
12	fmep0 (N indep friction k	1.01
13	Pacc (accessory - kW)	0.73
14	fmep1 (N dependent fric)	0.39

RANK	Parameter	Error Hwy
1	P/T indicated eff (eta)	8.52
2	Cd (drag coeff)	3.47
3	A (frontal area m^2)	3.47
4	Vehicle wgt (kg)	2.35
5	Cr0 (rolling resistance)	2.21
6	Engine Displ (L)	2.08
7	fmep0 (N indep friction k	1.81
8	overall motor efficiency	0.61
9	fmep1 (N dependent fric)	0.49
10	Pacc (accessory - kW)	0.44
11	Regen Brake Eff	0.30
12	FWD power frac	0.30
13	torq curve up 10%	0.24
14	Motor peak power (kW)	0.05

A sensitivity analysis is not conducted on the fuel cell hybrid, however, it is obvious from the above two studies that the fuel cell system efficiency curve is the most important parameter. The fuel cell peak power also being of moderate importance.

Road Load and Track Coefficients

Finally a brief comparison was run between using the road load coefficients Cr, Cd, A (area), etc, vs using the track (or target) coast-down coefficients (A, B, C). The fuel consumption was compared using both techniques for the conventional and hybrid vehicles. This is essentially a sensitivity analysis of the B term. It was found that the choice of methods made little difference for city fuel consumption results, but were significant for highway. For the city, the fuel consumption was underpredicted by about 2% (or less). For the highway cycle, the fuel consumption was underpredicted by 5% for conventional vehicles and 8% for hybrids on average. This implies that at high speed, the load curves from the estimated coefficients tend to be lower than those measured on the track. This could be due to the lack of a first order speed dependent term (B in force units), which tends to be quite small (or sometimes negative) on track tests. Additionally, there could be higher order rolling resistance terms [Gillespie, 1992]. It may be further aggravated in hybrids because of motor drag and their lack of a true neutral gear.

With production vehicles, the issue of choosing the method of calculating road loads is simple, since most of the track A, B, C coefficients are publicly available. Unfortunately, this cannot be done with vehicles, which have not yet been produced. It is impractical to combine Equations 1

and 3 in order to back-derive physical quantites from track A, B, and C coefficients, since the values are determined from empirical fits to coastdown data. Thus, it is necessary to have a methodology for estimating the effect of the B coefficients for future vehicles. Two methods of estimating its magnitude are compared here. The first method involves fitting to the known parameters.

The following coast-down force equations are based on Equations 1 and 3:

$$F_{RL} = mgC_R + 0.5\rho C_D A_r v^2 \quad (13)$$

$$F_T = A + Bv + Cv2 \quad (14)$$

Where the subscripts "RL" and "T" stand for "Road load" and "Track" respectively.

The equations are compared for the validation vehicles in the study. Then a B "correction" term is added into Equation 13 and empirically fitted to 14.

$$F_{RL} = mgC_R + Bv + 0.5\rho C_D A_r v^2 \quad (15)$$

The second method is to use the higher order rolling resistance term from Gillespie [1992] modified slightly here:

$$C_R = C_{R0}*(1+v/44.7) \quad (16)$$

Where C_{R0} is the base rolling resistance (typically ~.009). An estimate of B is

$$B' = MgC_{R0}/44.7 \quad [N/mps] \quad (17)$$

The speed dependent parameter in the denominator is not precise. It is estimated to double the rolling resistance factor at 100 mph. In other references, the speed dependent rolling resistance is embedded in the C parameter [Petrushov, 1997]. Unfortunately, this approach does not take other vehicle (non-tire) frictional factors into account.

Table 7 shows the fitted B coefficients along with their 1 standard deviation uncertainties. The third column displays the percentage underprediction in fuel consumption from the use of the road load Equation 1 compared to using the track Equation 3. The last column (B') shows the estimated value of B using Gillespie's method. First it is clear that the B term has a significant effect on fuel consumption. In all but the Camry, the difference is over 5% on the highway cycle. Comparing the fitted B with the estimated B', there is some agreement, but the trends break down for certain vehicles (e.g. Camry). Unfortunately, the tires (and rolling resistance) used for testing these vehicles were unknown. Moreover, the lack of correlation with some vehicles only supports the notion that other factors are inherent to the B term, such as rotating friction in bearings, transmission, and final drive, tire windage, motor drag etc. Because of the motor drag (and other hybrid differences), the official fuel economy numbers for certain hybrids may not necessarily match what one would achieve in the real world [Rechtin, 2003].

Table 7. Fitted B coefficients and 1 standard deviation. CV = Conventional Vehicle, HEV = Hybrid Electric Vehicle.

	B fit (N/mps)	sigma	HWY Fuel Cons Effect %	B'
Civic DX	2.01	0.19	8.60	2.44
Camry	0.67	0.07	1.48	3.09
Jetta	2.85	0.11	8.87	2.89
Civic hybrid	2.32	0.11	8.18	2.37
Insight	1.37	0.15	6.27	1.73
Prius 01	3.11	0.35	10.46	2.13
avg CV	**1.84**	**0.13**	**6.31**	**2.81**
avgHEV	**2.27**	**0.20**	**8.30**	**2.08**
avg ttl	**2.06**	**0.16**	**7.31**	**2.44**

This subject clearly requires further research. However, if a vehicle's A, B, C track coefficients are unknown, PERE will assume Gillespie's methodology, until an improved methodology is presented.

The subjects of dynamometer, track, and road load coefficients are complex. This brief study, only begins to scratch at the surface. A more full discussion of this topic is beyond the scope of this report.

Application to MOVES

PERE has been developed fundamentally to produce energy consumption and emission rates for MOVES for vehicle categories (known as "source bins" in MOVES terminology) where in-use data is insufficient to populate these rates directly. Thus PERE will produce these rates for most of the advanced technology vehicles (the focus of this report). The potential for PERE to compliment MOVES in this way is discussed in EPA [2002 -MOVES GHG emission analysis report].

Presently PERE is a standalone spreadsheet model capable of modeling on a finer scale than MOVES requires. PERE also has the potential to model a wider assortment of technologies than MOVES currently has. For example, PERE modeled a fuel cell hybrid with an ultracapacitor (above), but this particular technology is not modeled in MOVES. This flexibility allows for more source bins to be filled in the future as the need arises. However, the development time for each technology type using PERE is significant, so MOVES will model some advanced technologies directly using energy and emissions rates measured from other studies (e.g. hydraulic hybrids and some alternative fuels).

The process of how PERE results could be integrated into MOVES is the subject of this section. The final procedure is still subject to change, but fundamentally consists of the following steps:

Step 1: Choose the Source Bin

The first step is to determine what kind of vehicle PERE will model. In MOVES, these are defined by "source bins" defined by vehicle characteristics which differentiate energy consumption and emissions. For energy consumption, source bins have 5 dimensions: fuel type, engine technology, model year group, engine size, and loaded weight [Beardsley et al., 2004]. An example of some of the combined fuel types and engine technologies to be included in MOVES are in Table 8, along with the primary source of the energy consumption rates. PERE will be used to fill a majority of these technologies, but not all. In other cases, energy rates will be derived from already-published analyses. While this report focuses on light-duty, heavy-duty applications will be modeled as well with a version of PERE currently under development based on the principles presented in this report.

Table 8. Examples of advanced technologies, as defined by fuel types and engine technologies,to be included in MOVES. "C" is conventional, "A" is advanced, and "IC" is internal combustion. This list is not final.

- **Gasoline conventional (IC)**
- **Gasoline Advanced IC**
- **Gasoline Hybrid -CIC Mild**
- **Gasoline Hybrid -CIC Full**
- **Gasoline Hybrid -AIC Mild**
- **Gasoline Hybrid -AIC Full**
- **Diesel Fuel conventional (IC)**
- **Diesel Fuel Advanced IC**
- **Diesel Fuel Hybrid -CIC Mild**
- **Diesel Fuel Hybrid -CIC Full**
- **Diesel Fuel Hybrid -AIC Mild**
- **Diesel Fuel Hybrid -AIC Full**
- **Compressed Natural Gas (CNG) conventional (IC)**
- **Liquid Propane Gas (LPG) conventional (IC)**
- **Ethanol (E85 or E95) conventional (IC)**
- **Methanol (M85 or M95) conventional (IC)**
- **Gaseous Hydrogen Advanced IC**
- **Hydrogen -Fuel Cell**
- **Hydrogen Hybrid -Fuel Cell**
- **Electricity electric only**

Not all of the engine technologies are represented fully across the other 5 dimensions, for example, it is highly unlikely that long haul trucks will be hybridized in the future, due to the relatively minor effect it has on highway fuel economy compared to the already efficient diesels. However, hybridization is quite promising for buses. Due to the sheer number of tests required, simplifications are necessary. Examples of these are described in greater detail below.

Step 2: Define the Vehicle Specifications

Based on the engine technology source bin, the vehicle parameters such as weight, engine size, vehicle shape etc, can be defined. The weight and engine size values are simply the central value

of the bin. Thus PERE effectively models an "average" vehicle in the source bin. For the source bins on the "edge" of the matrix (<2000 lbs; >130,000lbs; <2.0L; and >5.0L), their results will be extrapolated - see Step 6.

Since engine size, has limited meaning for hybrids and no meaning for fuel cells, it is necessary to define a power surrogate for engine size. This has already been mentioned in this report [Chon and Heywood, 2000]. Though it is not perfect, we will take the convention that motor power + engine peak power = total peak power. The fuel cell definition of power is simpler since there is only one motor and the battery and fuel cell should be sized optimally within the motor limitations.

Because the source bins do not have a dimension for body type, the estimations for will be estimated based on the weight. Lighter light duty weights tend to be (compact) passenger cars, then midsize cars, luxury, compact pickups, SUVs, minivans on up to medium light duty trucks (heavy-duty trucks are discussed in a separate report). The variation in body types will certainly lead to variation (or uncertainty) in the emission rates.

Step 3: Run PERE on the FTP if Modeling a Hybrid

Once the vehicle specifications have been finalized for the source bin, the next step is to run the model over the FTP driving cycle (city and highway). This is to determine the hybrid threshold for charge sustaining. It also gives the estimated fuel economy of the vehicle. If a hybrid is not modeled, or if fuel economy is not required, this step can be skipped.

Step 4: Define the Driving Cycles

The output to PERE is second-by-second energy consumption, therefore the next step is to input the driving cycles. The driving cycles input into PERE help determine the "binned" energy consumption rates for MOVES (see Figure 1). Henceforth "binned" refers to operating mode bin and not source bin, which has already been defined.

The binned energy consumption and emissions rates are dependent on the driving cycle input. It is important to capture a representative sampling of real-world driving. 14 driving cycles for light duty applications have been selected for this purpose from MOVES. These cycles represent a broad spectrum of driving, from very low to very high speeds. The cycles and their average speeds are shown on Table 9. When merged, the cycles run 6,981 seconds. It is also important to artificially set the accelerations to zero in between the cycles since they do not all start from rest.

Table 9. The 14 MOVES light-duty driving cycles used as input to PERE.

CYCLE	avg spd
FWYHI1	63.2
FWYAC	59.7
FWYD	52.9
FWYE	30.5
FWYF	18.6
FWYG	13.1
RAMP	n/a
ARTAB	24.8
ARTCD	19.2
ARTEF	11.6
NYCC	7.1
FWYHI2	68.2
FWYHI3	76.0
LOWSPEED1	2.5

It should be noted that for hybrids, the change in driving cycles may not necessarily maintain the battery state of charge.

Step 5: Run PERE and Bin Output

After PERE is run, the rates must be binned into the respective operating modes. These are the 17 VSP and speed operating mode bins as defined in Koupal [2003]. The binning procedure is straightforward and can be programmed in any script.

Figure 19 shows a sample of predicted fuel consumption as a function of VSP for a fictional hybrid passenger car. This is an indication of how an output from PERE would be translated into an emissions rate in MOVES. The uncertainty bars are from PERE generated variations within a bin, and do not adequately reflect the true uncertainty of the emission rates, which will be added in future versions of PERE.

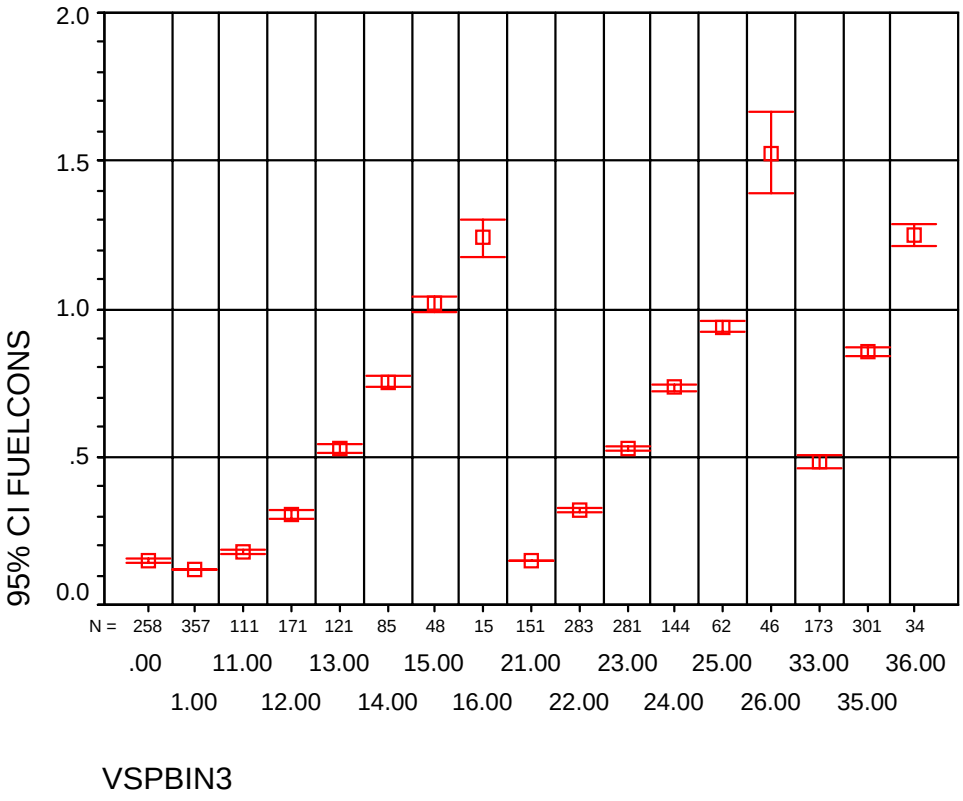

Figure 19. Hybrid fuel consumption as a function of VSP bin.

Step 6: Repeat for the Rest of the Source Bins

Rather than run PERE for every operating mode bin within every advanced technology source bin, it is more efficient to extrapolate from one bin to another along a dimension. A dimension could be weight or power (engine displacement), so the rates could be interpolated between the endpoints (e.g. lightest and heaviest weight class. To demonstrate the validity of the linear extrapolation technique, PERE was run on a conventional gasoline powered passenger car for a variety of weights and engine displacements. The driving cycles employed were the city and highway portions of the FTP. The base car is a 3500lb, 2.5L passenger car. For the different engine sizes, the VSP values are identical, however, this is not true along the weight axis. Here the second-by-second fuel consumption as well as the VSP values are binned.

Figure 20 shows the fuel consumption rates as a function of VSP bin. Each color represents a separate engine displacement, as labelled along the right. It is evident that given the minimum and maximum points, that the other could be linearly interpolated.

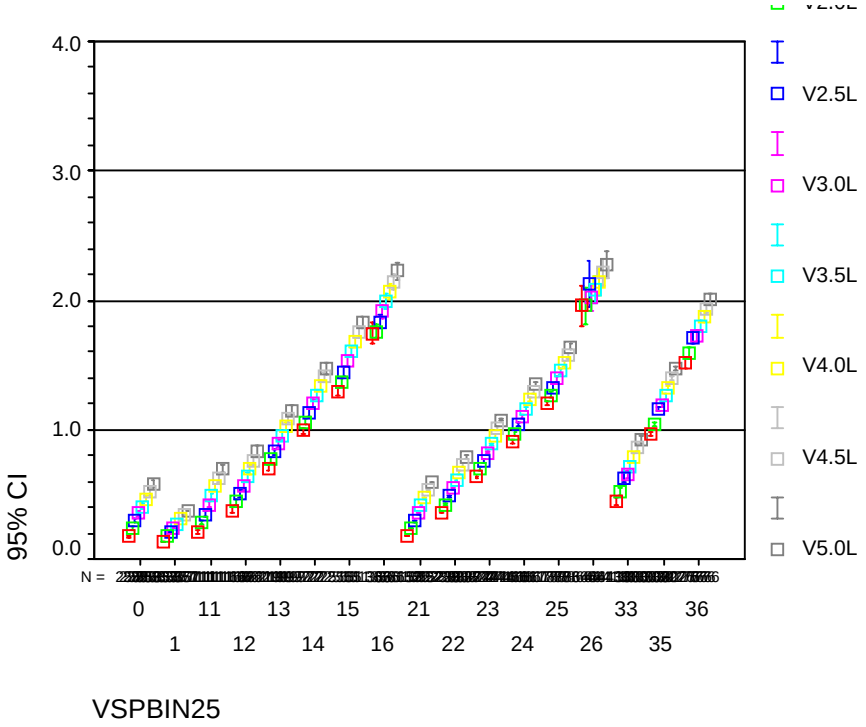

Figure 20. Fuel Rate (g/s) as a function of VSP bin for engine sizes 1.5 – 5.0L.

Figure 21 shows the same relationship but with vehicle weight varied instead of engine displacement. Despite the curvature between the VSP bins, within a bin, an interpolation is quite reasonable.

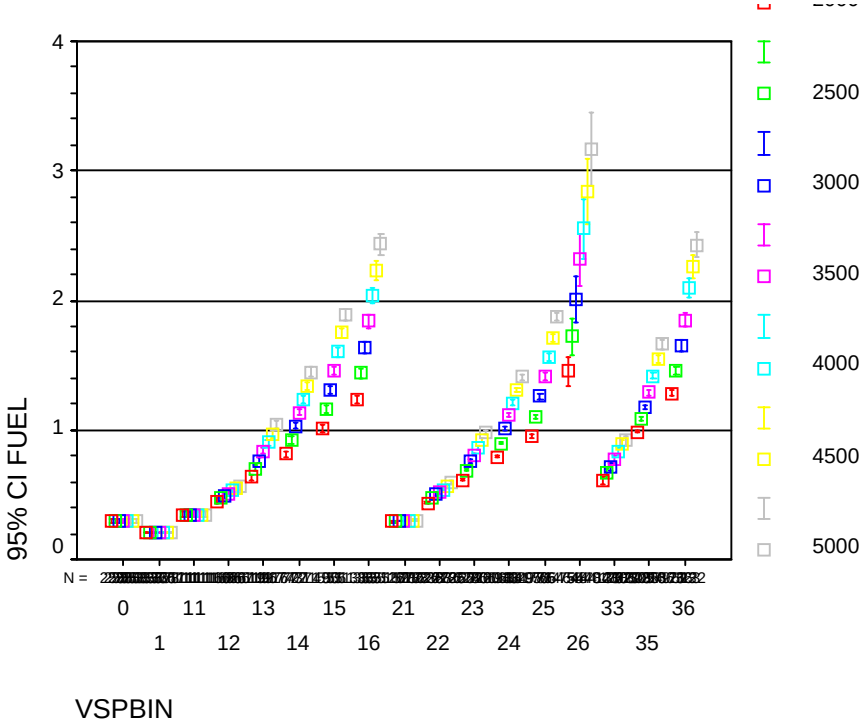

Figure 21. Fuel Rate (g/s) as a function of VSP bin for weights ranging from 2000 – 5000 lbs.

Given the rates in any two cells near the edge of the matrix, the rest of the emission rates can be interpolated or extrapolated. Figure 22 shows a matrix and defines an example bin filling strategy. The red bins are possible engine size (power) and weight combinations. The green bins are filled using PERE and the black arrows represent the direction of interpolation or extrapolation. The rest of the bins can be filled interpolating from the edge bins. In this case, PERE needs to be run a minimal of four times. Note that each of the bins below has 17 operating mode bins to fill.

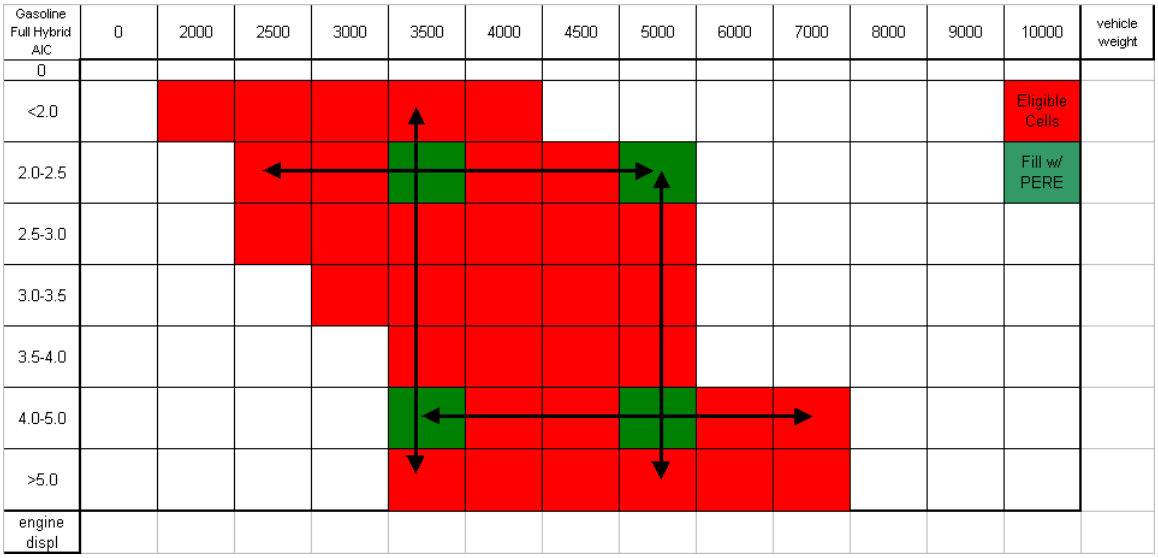

Figure 22. A sample source bin matrix hole filling strategy.

When choosing bins to fill, the absolute edge bins (<2000 lbs; >130,000lbs; <2.0L; and >5.0L) should not be run since the masses and or engine sizes are not well defined. This is the reason for choosing the "outer" bins in Figure 22, but not the "edge" bins.

If it is easier to fill each bin with PERE, rather than interpolating, this can also be done.

Step 7: Insert Estimated Cold Start Energy/Emission Factors
This is discussed in more detail in the next section. Cold start factors will be approximated within MOVES, not PERE.

Cold Start

Modern vehicles are capable of eliminating nearly all of the criteria pollutants during hot running periods. However, during cold starts, the engine and the catalytic converter are cold, thus preventing the breakdown of emissions. For the vehicles meeting the cleanest standards, the cold start emissions account for most of the vehicle's operating emissions. However, the impact on fuel consumption is not as dramatic.

Due to the lack of data on which to base a model, cold start fuel consumption factors are still elusive for advanced technology vehicles. However, there are steps PERE can take in order to estimate the effects of cold start.

In order for criteria pollutants to be treated in the catalytic converter, the catalyst must first obtain a high enough temperature to break down the pollutants. Before this can happen, the engine must warm up to a point where its exhaust is hot enough to heat the catalyst. When this temperature is reached, this condition is referred to as “light-off”. In order for the catalyst to light-off, the heat from the engine exhaust must heat the catalyst, therefore the engine must be running until this point. At this time, PERE cannot predict at what time light-off will occur, this must be done empirically. Typical gasoline vehicles light-off somewhere around 2 minutes into the first portion (bag 1) of the FTP. There are advanced technologies, which help minimize this light-off time, but they usually come at a cost. For example, the engine may run rich briefly, or electrical power may be needed to pre-heat the catalyst. In either of these cases, energy is being consumed. Additionally, the engine runs less efficiently while it is cold.

In PERE, the fuel strategy on the full hybrid vehicle (used in the sensitivity study) is adjusted so that the engine remains on for the first 2 minutes of the test. The battery power is set to zero for the duration, so that vehicle is acting much like a conventional vehicle, with the exception that the regenerative brakes are still active. The fuel never goes to zero in this scenario, but is minimal at engine idle. The additional energy (fuel) consumed in this period is assumed to balance any alternative technologies such as electrically heated catalyst.

The fuel consumption from this modified hybrid vehicle increases by 3.2% on the city cycle, while the fuel economy decreases by 3.1%. This corresponds to 11% fuel consumption increase on bag 1 vs bag 3 (10% lower fuel economy). This is likely to be a conservative estimate to use for the model. By subtracting the hot running bag 3 from the bag 1, this corresponds to a cold start factor of 22.3 grams of fuel per start. This start factor will depend on the type of hybrid, size of engine, and other vehicle parameters. It is hoped that in time, data will be collected, which can improve upon this estimate. Kim and Lee [2004] measured the cold vs hot fuel economy for the (pre-2004) Toyota Prius. Their report indicates that the city cold start fuel economy was 12.4% worse than a hot start test. However, their test vehicle may have had a different calibration than one in the United States.

Including cold start, the efficiency could be improved over the one mentioned above. It would be advantageous to run the engine at higher loads during the cold start period. This serves the 3-fold advantage of heating up the catalyst quickly, running the engine at a more efficient mode, and recharging the batteries so that more of the rest of the cycle can be run on electrical power alone. Since the light-off time would be shortened, the cold start fuel consumption factor may not increase significantly.

Acknowledgments

The author would like to thank the following people for the help and support: Bob Giannelli, John Koupal, Joe McDonald, James Warila, and and Tad Wysor from the EPA. Also Feng An and Dan Santini from Argonne National Laboratory for their valuable feedback.

References

Alson, J., D. Barba, J. Bryson, M. Doorlag, D. Haugen, J. Kargul, J. McDonald, K. Newman, L. Platte, M. Wolcott, "Progress Report on Clean and Effective Automotive Technologies Under Development at EPA," EPA document number: EPA420-R-04-002, 2004.

An, F., and M. Ross, "The Use of Fuel by Spark Ignition Engines," SAE 930329, 1993.

An, F., D.,J. Santini, "Mass Impacts on Fuel Economies of Conventional vs. Hybrid Electric Vehicles," SAE 2004-01-0572, 2004.

Beardsley, M., D. Brzezinski, R. Gianelli, J. Koupal, S. Srivastava, "MOVES 2004: 1999 Highway Vehicle Population and Activity Data," EPA Document to be published, 2004.

Barth, M., F. An, T. Younglove, G. Scora, C. Levine, M. Ross, T. Wenzel, "Comprehensive Modal Emission Model (CMEM), version 2.0 User's Guide," 1999.

Bishop, J.S., M.A. Kluger, "Proposed Efficiency Rating for Automatic Transmissions," SAE 960425, 1996**.**

Bosch, "Automotive Handbook – 5th Edition," Stuttgart, Robert Bosch GmbH, 2000.

Car and Driver Website: www.caranddriver.com

Chon, D.M., J.B. Heywood, "Performance Scaling of Spark-Ignition Engines: Correlation and Historical Analysis of Production Engine Data," SAE 2000-01-0565, 2000.

DaimlerChrysler publication: "F-Cell, Driving the Future," October, 2003. (http://www.mercedes-benz.com/com/e/home/innovation/laboratory/fuelcell/impraxistest/aclassfcell/index2.html)

Ford Motor Company pamphlet, "Ford Focus Hydrogen Fuel Cell Electric Vehicle," 2003

General Motors pamphlet, "Hydrogen 3, GM Fuel Cell Technology," 2003.

General Motors News Website: "GM's Hybrid Timeline," http://www.gm.com/company/gmability/adv_tech/300_hybrids/hyb_timeline.html, 2004

Gillespie, T., "Fundamentals of Vehicle Dynamics," Society of Automotive Engineers, 1992.

Goodwin, R.W., M. Ross, "Off-Cycle Exhaust Emissions from Modern Passenger Cars with Properly-Functioning Emissions Controls," SAE 960064, 1996.

Greenbaum, J.J., M.A. Kluger, B.E. Westmoreland, "Manual Transmission Efficiency Trends and Characteristics," SAE 942274, 1994.

Heywood, J.B., "Internal combustion engine fundamentals," McGraw-Hill, New York, 1998.

Honda Motor Company publication (pamphlet): “FCX Fuel Cell Power

Honda Motor Company website: “Remarks by Takeo Fukui, President and CEO, Honda Motor Co., Ltd. -- North American International Auto Show,” http://www.hondacars.com/info/news/article.asp?ArticleID=2004010562646&Category=currenthonda, 2004

Jimenez-Palacios, J., “Understanding and Quantifying Motor Vehicle Emissions with Vehicle Specific Power and TILDAS Remote Sensing,” PhD Thesis, Massachusetts Institute of Technology, Cambridge, MA, 1999.

Kelly, K.J., M. Zolot, G. Glinsky, A. Hieronymous, “Test Results and Modeling of the Honda Insight using ADVISOR,” SAE 2001-01-2537.

Kluger, M.A., J.J. Greenbaum, D.R. Mairet, “Proposed Efficiency Guidelines for Manual Transmissions for the Year 2000,” SAE 950892, 1995.

Koupal, J., “Emission Rate Development,” Presentation at FACA technical review meeting Dec 2, 2003, Ann Arbor, MI.

Laramie, J., A. Dicks, “Fuel Cell Systems Explained,” John Wiley & Sons Ltd., West Sussex, England, 2000.

Milington, B.W., E.R. Hartles, “Frictional Losses in Diesel Engines,” SAE 680590, 1968.

Muranaka, S., Y. Takagi, T. Ishida, “Factors Limiting the Improvement in Thermal Efficiency of S.I. Engine at Higher Compression Ratio,” SAE 870548, 1987

Nam, E.K., J. Sorab, “Friction Reduction Trends in Modern Engines,” SAE 2004-01-1456, 2004.

Nam, E.K., “Proof of Concept Investigation for the Physical Emission Rate Estimator (PERE) for MOVES,” EPA document number: 420-R-03-005, February, 2003.

Nelson, D.J., “Automotive Fuel Cell Systems,” Lecture Slides, Society of Automotive Engineers, 2003.

Ogawa, H., M. Matsuki, T. Eguchi, “Development of a Power Train for the Hybrid Automobile – The Civic Hybrid,” SAE 2003-01-0083.

Pachernegg, S.J., “A Closer Look at the Willans-Line,” SAE 690182, 1969.

Park, D.H., T.S. Seo, D.G. Lim, H.B. Cho, “Theoretical Investigation on Automatic Transmission Efficiency,” SAE 960426, 1996.

Patton, K.J., R.G. Nitschke, J.B. Heywood, “Development and Evaluation of a Friction Model for Spark-Ignition Engines,” SAE 890836, 1989.

Petrushov, V.A., “Coast Down Method in Time-Distance Variables,” SAE 970408, 1997.

Rechtin, M., “EPA mpg test doesn’t work for hybrids,” Automotive News, November 24, 2003.

Road and Track website: www.roadandtrack.com

Ross, M., “Fuel Efficiency and the Physics of Automobiles,” Contemporary Physics, vol. 38, number 6, pp 381-394, 1997.

Sandoval, D., J.B. Heywood, “An Improved Friction Model for Spark Ignition Engines,” SAE 2003-01-0725, 2003.

Schaefer, R.M., “Testing of an Electric Vehicle on a Clayton Water-Brake Chassis Dynamometer,” EPA document: EPA/AA/TDG/94-01, 1994.

Thomas, M., M. Ross, “Development of Second-by-second Fuel Use and Emissions Models Based on an Early 1990s Composite Car,” SAE 971010, 1997.

Toyota Motor Coporation, “Toyota FCHV Book,” Tokyo, Japan. March, 2003.

Toyota Motor Coporation, Public Affairs Division, “Toyota Hybrid System, THS II,” Tokyo, Japan, May 2003.

Toyota Motor Coporation Press release: “Toyota Stages World Premiere of All-new Highlander Hybrid SUV at 2004 North American International Auto Show,” website: http://www.toyota.co.jp/en/event/auto_shows/2004/naias/toyota_suv.html, 2004

U.S. Department of Energy, U.S. Environmental Protection Agency, “Fuel Economy Guide,” 2004. (www.fueleconomy.gov)

Weiss, M.A., J.B. Heywood, E.M. Drake, A. Schafer, F.F. AuYeung, “On the Road in 2020 – A Life Cycle Analysis of New Automobile Technologies,” Massachusetts Institute of Technology Energy Laboratory Report # MIT EL 00-003. October, 2000.

Weiss, M.A., J.B. Heywood, A. Schafer, V.K. Natarajan, “Comparitive Assessment of Fuel Cell Cars,” Massachusetts Institute of Technology Energy Laboratory Report # MIT LFE 2003-001 RP. February, 2003.

Wu, W., M. Ross, “Modeling of Direct Injection Diesel Engine Fuel Consumption,” SAE 971142, 1997.

Yagi, S., Y. Ishibasi, H. Sono, “Estimation of Total Engine Loss and Engine Output in Four Stroke S.I. Engines,” SAE 900223, 1990.

Appendix A: PERE Algorithms

Key:

FR	Fuel rate (g/s)
KNV	Friction term
LHV	Lowere heating value of fuel
P_{acc}	Accessory power
P_{batt}	Battery power
P_d	Power demand
P_{eng}	Engine power
P_{FC}	Fuel Cell power
P_{engmax}	Maximum power of engine
P_{fcmax}	Maximum power of fuel cell
P_{motmax}	Maximum power of motor
P_{min}	Minimum regeneration power
P_{mot}	Motor power
P_{th}	Hybrid threshold power
η	Engine indicated efficiency
η_{disch}	Battery discharge efficiency
η_{FC}	Fuel cell efficiency
η_{FD}	Final drive efficiency (for motor only)
η_{FWD}	Front wheel drive power fraction
η_{mot}	Motor efficiency
η_{tran}	Transmission efficiency
η_{regen}	Regenerative braking recharge efficiency

Parallel Hybrid Algorithm

Engine Power (nested if statements)

IF OR($v < 2$, $P_d < P_{th}$) THEN $P_{eng} = 0$ ‘idle & decel engine shut-off

IF $P_d > P_{engmax}$ THEN $P_{eng} = P_{engmax}$ ‘can’t exceed max

ELSE $P_{eng} = P_d$

Fuel Rate

IF $P_d = 0$ THEN FR = 0 ‘fuel shut-off

IF $P_d > P_{engmax}$ THEN FR = [KNV + $P_{eng} / \eta\eta_{tran}$]/LHV ‘no P_{acc} – slightly overpower

ELSE FR = [KNV + ($P_{eng} / \eta_{tran} + P_{acc}$)/$\eta$]/LHV

Battery discharge ($P_{batt} > 0$)

IF AND($P_d <= P_{th}$, $P_d > 0$) THEN $P_{batt} = (P_d / \eta_{mot}\eta_{FD} + P_{acc})/\eta_{disch}$ ‘launch

IF $P_d > P_{engmax} + P_{motmax}$ THEN $P_{batt} = P_{motmax}$ ‘can’t exceed max

IF $P_d > P_{engmax}$ THEN $P_{batt} = [(P_d - P_{engmax})/\eta_{mot}\eta_{FD} + P_{acc}]/\eta_{disch}$ ‘assist

ELSE $P_{batt} = 0$

Battery recharge ($P_{batt} < 0$)

IF $P_d <= - P_{motmax}/\eta_{FWD}$ THEN $P_{batt} = -P_{motmax}\eta_{mot}\eta_{regen}\eta_{FD}$ ‘can’t exceed max

If $P_d < - P_{min}/\eta_{FWD}$ THEN $P_{batt} = P_d\eta_{FWD}\eta_{mot}\eta_{regen}\eta_{FD}$ ‘can’t fall below min

ELSE $P_{batt} = 0$

Fuel Cell Hybrid Algorithm

Fuel Cell Powerplant

IF OR($v < 2$, $P_d < P_{th}$) THEN $P_{FC} = 0$ ‘idle & decel fc shut-off

IF $P_d > P_{motmax}$ THEN $P_{FC} = P_{fcmax}$ ‘can’t exceed max

ELSE P $P_{FC} = [P_d/(\eta_{mot}\eta_{FD}) + P_{acc}]/\ \eta_{FC}$

Battery (ultracapacitor) discharge

IF AND($P_d <= P_{th}$, $P_d > 0$) THEN $P_{batt} = (P_d/\eta_{mot}\eta_{FD} + P_{acc})/\eta_{disch}$ ‘launch

IF AND ($P_d > P_{fcmax}$, $P_d < P_{motmax}$) THEN $P_{batt} = [(P_d – P_{fcmax})/\eta_{mot}\eta_{FD} + P_{acc}]/\eta_{disch}$

IF $P_d <= 0$ THEN $P_{batt} = P_{acc}/\eta_{disch}$

ELSE $P_{batt} = 0$

Battery recharge

Same as for hybrid (above)

Appendix B: Tables of parameters for validation vehicles.

Vehicle	MIT	Camry	Jetta	Jetta TDI	Civic DX	Civic HX	Civic Hybrid	Insight	Prius '01	Prius '04
Model Year	2020	2004	2004	2004	2004	2004	2004	2004	2001	2004
Vehicle wgt (kg)	1154	1565	1467	1483	1239	1224.2664	1354	989	1390	1447
Cr0 (rolling resistance)	0.006	0.009	0.009	0.009	0.009	0.009	0.008	0.008	0.009	0.007
Cd (drag coeff)	0.22	0.3	0.3	0.3	0.3	0.3	0.28	0.26	0.26	0.26
A (frontal area m^2)	1.8	2.4	2.11	2.11	2.14	2.14	2.14	1.92	2.11	2.33
Pacc (accessory - kW)	1	0.75	0.75	0.75	0.75	0.75	0.75	0.75	0.75	0.75
A (N)		127.36	111.25	111.25	105.47	105.47	125.58	53.76	86.33	88.63
B (N/mps)		0.9578	3.6834	3.6834	5.4276	5.4276	-0.9000	2.2837	2.2355	1.3849
C (N/mps^2)		0.4374	0.3764	0.3786	0.2670	0.2670	0.4474	0.3013	0.4144	0.3645
Engine										
Engine Displ (L)	1.11	2.4	2	1.9	1.7	1.7	1.35	1	1.5	1.5
k0 (N indep friction kJ/Lrev)	0.153	0.164	0.164	0.123	0.164	0.15088	0.15088	0.15088	0.164	0.164
k1 (N dependent fric)	0.00155	0.00155	0.00155	0.00215	0.00155	0.00155	0.00155	0.00155	0.00155	0.00155
P/T indicated eff (eta)	0.405	0.405	0.405	0.45	0.405	0.48	0.48	0.48	0.46575	0.46575
Transmission										
N/v (rpm/mph)	35.6	35.6	35.6	26.7	35.6	35.6	35.6	35.6	35.6	35.6
Nidle (rpm)	700	700	700	700	700	700	700	700	700	700
trans eff	0.88	0.88	0.88	0.88	0.88	0.88	0.88	0.88	0.88	0.88
Shift point 1-2 (mph)	18	18	18	18	18	15	18	18	18	18
Shift point 2-3	25	25	25	25	25	25	25	25	25	25
Shift point 3-4	40	40	40	40	40	40	40	40	40	40
Shift point 4-5	50	50	50	50	50	50	50	50	50	50
g/gtop 1	4.04	4.04	4.04	4.04	4.04	4.04	4.04	3.461	4.04	4.04
g/gtop 2	2.22	2.22	2.22	2.22	2.22	2.22	2.22	1.75	2.22	2.22
g/gtop 3	1.44	1.44	1.44	1.44	1.44	1.44	1.44	1.096	1.44	1.44
g/gtop 4	1.00	1.00	1.00	1.00	1.00	1	1.00	0.86	1.00	1.00
g/gtop 5	0.90	0.90	0.90	0.90	0.90	0.9	0.90	0.71	0.90	0.90
Fuel										
LHV (kJ/g)	43.7	43.7	43.7	41.7	43.7	43.7	43.7	43.7	43.7	43.7
density gas (kg/L)	0.737	0.737	0.737	0.856	0.737	0.737	0.737	0.737	0.737	0.737
Motor										
overall efficiency	0.76						0.76	0.76	0.76	0.76
Regen Brake Eff	0.85						0.85	0.85	0.85	0.85
FWD power frac	0.7						0.75	0.75	0.7	0.95
Motor peak power (kW)	30						10	10	33	50
min regen (kW)	2.8						2.8	2.8	2.8	2.8
Motor Energy (kWhr)	1.8						1.8	1.8	1.8	1.8
Battery										
Initial SOC	0.56						0.56	0.56	0.56	0.56
Batt Energy (kWh)	1.8						0.936	0.936	1.8	1.3104
min SOC	0.2						0.2	0.2	0.4	0.4
max SOC	0.8						0.8	0.8	0.8	0.8
discharge eff	0.95						0.95	0.95	0.95	0.95
Hybrid										
hybrid threshold (kW)	1.75						2.2	1.5	2.18	2.9